Umetani K, Ueki H, Yokoyama T, Tanioka K, Kubota M, Hosaka H, Ishikawa N, Ando M. Small-vessel radiography in situ with monochromatic synchrotron radiation. *Radiology*. 1996;201:173–177.
17. White FC, Carroll SM, Magnet A, Bloor CM. Coronary collateral development in swine after coronary artery occlusion. *Circ Res*. 1992;71:1490–1500.
18. Unger EF, Banai S, Shou M, Lazarous DF, Jaklitsch MT, Scheinowitz M, Correa R, Klingbeil C, Epstein SE. Basic fibroblast growth factor enhances myocardial collateral flow in a canine model. *Am J Physiol*. 1994;266:H1588–1595.
19. Takeshita S, Rossow ST, Kearney M, Zheng LP, Bauters C, Bunting S, Ferrara N, Symes JF, Isner JM. Time course of increased cellular proliferation in collateral arteries after administration of vascular endothelial growth factor in a rabbit model of lower limb vascular insufficiency. *Am J Pathol*. 1995;147:1649–1660.
20. Rubenstein E, Hofstadter R, Zeman HD, Thompson AC, Otis JN, Brown GS, Giacomini JC, Gordon HJ, Kernoff RS, Harrison DC, et al. Transvenous coronary angiography in humans using synchrotron radiation. *Proc Natl Acad Sci U S A*. 1986;83:9724–9728.
21. Mori H, Tanaka E, Hyodo K, Uddin Mohammed M, Sekka T, Ito K, Shinozaki Y, Tanaka A, Nakazawa H, Abe S, Handa S, Kubota M, Tanioka K, Umetani K, Ando M. Synchrotron microangiography reveals configurational changes and to-and-fro flow in intramyocardial vessels. *Am J Physiol*. 1999;276:H429–H437.
22. Takeshita S, Isshiki T, Mori H, Tanaka E, Eto K, Miyazawa Y, Tanaka A, Shinozaki Y, Hyodo K, Ando M, Kubota M, Tanioka K, Umetani K, Ochiai M, Sato T, Miyashita H. Use of synchrotron radiation microangiography to assess development of small collateral arteries in a rat model of hindlimb ischemia. *Circulation*. 1997;95:805–808.
23. Tanaka E, Tanaka A, Sekka T, Shinozaki Y, Hyodo K, Umetani K, Mori H. Digitized cerebral synchrotron radiation angiography: quantitative evaluation of the canine circle of Willis and its large and small branches. *Am J Neuroradiol*. 1999;20:801–806.
24. Sekka T, Volchikhina SA, Tanaka A, Hasegawa M, Tanaka Y, Ohtani Y, Tajima T, Makuuchi H, Tanaka E, Iwata Y, Sato S, Hyodo K, Ando M, Umetani K, Kubota M, Tanioka K, Mori H. Visualization, quantification and therapeutic evaluation of angiogenic vessels in cancer by synchrotron microangiography. *J Synchrotron Radiat*. 2000;7:361–367.
25. Kidoguchi K, Tamaki M, Mizobe T, Koyama J, Kondoh T, Kohmura E, Sakurai T, Yokono K, Umetani K. In vivo X-ray angiography in the mouse brain using synchrotron radiation. *Stroke*. 2006;37:1856–1861.
26. Gaipa G, Dassi M, Perseghin P, Venturi N, Corti P, Bonanomi S, Balduzzi A, Longoni D, Uderzo C, Biondi A, Masera G, Parini R, Bertagnolio B, Uziel G, Peters C, Rovelli A. Allogeneic bone marrow stem cell transplantation following CD34+ immunomagnetic enrichment in patients with inherited metabolic storage diseases. *Bone Marrow Transplant*. 2003;31:857–860.
27. Beaussier M, Mouren S, Souktani R, Arthaud M, Massias L, Vicaut E, Lienhart A, Coriat P. Role of nitric oxide and cyclooxygenase pathways in the coronary vascular effects of halothane, isoflurane and desflurane in red blood cell-perfused isolated rabbit hearts. *Br J Anaesth*. 2002;88:399–407.
28. Heitzer T, Baldus S, von Kodolitsch Y, Rudolph V, Meinertz T. Systemic endothelial dysfunction as an early predictor of adverse outcome in heart failure. *Arterioscler Thromb Vasc Biol*. 2005;25:1174–1179.
29. Becker A, Reith A, Napiwotzki J, Kadenbach B. A quantitative method of determining initial amounts of DNA by polymerase chain reaction cycle titration using digital imaging and a novel DNA stain. *Anal Biochem*. 1996;237:204–207.
30. Orlic D, Kajstura J, Chimenti S, Jakoniuk I, Anderson SM, Li B, Pickel J, McKay R, Nadal-Ginard B, Bodine DM, Leri A, Anversa P. Bone marrow cells regenerate infarcted myocardium. *Nature*. 2001;410:701–705.
31. Jackson KA, Majka SM, Wang H, Pocius J, Hartley CJ, Majesky MW, Entman ML, Michael LH, Hirschi KK, Goodell MA. Regeneration of ischemic cardiac muscle and vascular endothelium by adult stem cells. *J Clin Invest*. 2001;107:1395–1402.
32. Toyota E, Warltier DC, Brock T, Ritman E, Kolz C, O'Malley P, Rocic P, Focardi M, Chilian WM. Vascular endothelial growth factor is required for coronary collateral growth in the rat. *Circulation*. 2005;112:2108–2113.

CD34-Positive Cells Exhibit Increased Potency and Safety for Therapeutic Neovascularization After Myocardial Infarction Compared With Total Mononuclear Cells

Atsuhiko Kawamoto, MD, PhD; Hiroto Iwasaki, MD; Kengo Kusano, MD, PhD; Toshinori Murayama, MD, PhD; Akira Oyamada, BS; Marcy Silver, BS; Christine Hulbert, BS; Mary Gavin, BS; Allison Hanley, BS; Hong Ma, BS; Marianne Kearney, BS; Victor Zak, PhD; Takayuki Asahara, MD, PhD; Douglas W. Losordo, MD

Background—We compared the therapeutic potential of purified mobilized human $CD34^+$ cells with that of mobilized total mononuclear cells (tMNCs) for the preservation/recovery of myocardial tissue integrity and function after myocardial infarction (MI).

Methods and Results—$CD34^+$ cells were purified from peripheral blood tMNCs of healthy volunteers by magnetic cell sorting after a 5-day administration of granulocyte colony-stimulating factor. Phosphate-buffered saline (PBS), 5×10^5 $CD34^+$ cells/kg, 5×10^5 tMNCs/kg (low-dose MNCs [loMNCs]), or a higher dose of tMNCs (hiMNCs) containing 5×10^5 $CD34^+$ cells/kg was transplanted intramyocardially 10 minutes after the induction of MI in athymic nude rats. Hematoxylin and eosin staining revealed that moderate to severe hemorrhagic MI on day 3 was more frequent in the hiMNC group than in the PBS and $CD34^+$ cell groups. Immunostaining for human-specific CD45 revealed abundant distribution of hematopoietic/inflammatory cells derived from transplanted cells in the ischemic myocardium of the hiMNC group. Capillary density on day 28 was significantly greater in the $CD34^+$ cell group (721.1±19.9 per 1 mm^2) than in the PBS, loMNC, and hiMNC groups (384.7±11.0, 372.5±14.1, and 497.5±24.0 per 1 mm^2) ($P<0.01$). Percent fibrosis area on day 28 was less in the $CD34^+$ cell group (15.6±0.9%) than in the PBS, loMNC, and hiMNC groups (26.3±1.2%, 27.5±1.8%, and 22.2±1.8%) ($P<0.05$). Echocardiographic fractional shortening on day 28 was significantly higher in the $CD34^+$ cell group (30.3±0.9%) than in the PBS, loMNC, and hiMNC groups (22.7±1.5%, 23.4±1.1%, and 24.9±1.7%; $P<0.05$). Echocardiographic regional wall motion score was better preserved in the $CD34^+$ cell group (21.8±0.5) than in the PBS, loMNC, and hiMNC groups (25.4±0.4, 24.9±0.4, and 24.1±0.6; $P<0.05$).

Conclusions—$CD34^+$ cells exhibit superior efficacy for preserving myocardial integrity and function after MI than unselected circulating MNCs. (***Circulation*. 2006;114:2163-2169.**)

Key Words: angiogenesis ■ endothelium ■ ischemia ■ progenitor cells ■ stem cells

Since endothelial progenitor cells (EPCs) were identified as circulating CD34 antigen–positive mononuclear cells,[1] the therapeutic potential of purified EPCs or total (unpurified) mononuclear cells (tMNCs) containing both EPC and non-EPC fractions has been evaluated in many preclinical and clinical studies. Transplantation of purified EPCs augments ischemic neovascularization in mice with hind-limb ischemia,[2,3] rats with acute myocardial ischemia,[4,5] and swine with chronic myocardial ischemia.[6] Recent pilot clinical trials also have suggested the therapeutic potential of EPC transplantation in patients with coronary artery disease.[7,8] On the other hand, tMNC transplantation has been further reported. Trials using tMNCs have demonstrated their therapeutic efficiency

Clinical Perspective p 2169

to enhance ischemic neovascularization in animal studies[9,10] and human clinical trials.[11,12] Although tMNCs consist mainly (>99%) of non-EPCs and contribute to limited vasculogenic volume by EPCs, transplantation of the non-EPC fraction stimulates secretion of angiogenic cytokines in ischemic tissue.[10] However, the fate of the non-EPC fraction after transplantation into ischemic sites is not well known. The non-EPC fraction of hematopoietic cells might cause excess inflammation in the ischemic

Received March 3, 2006; de novo received June 8, 2006; revision received August 23, 2006; accepted September 8, 2006.

From the Division of Cardiovascular Research, St Elizabeth's Medical Center, Tufts University School of Medicine, Boston, Mass (A.K., K.K., T.M., M.S., C.H., M.G., A.H., H.M., M.K., V.Z., T.A., D.W.L.); Laboratory for Stem Cell Translational Research, Kobe Institute of Biomedical Research and Innovation/RIKEN Center for Developmental Biology, Kobe, Japan (A.K., H.I., A.O., T.A.); and Department of Regeneration Medicine Science, Tokai University School of Medicine, Isehara, Japan (T.A.).

Correspondence to Takayuki Asahara, MD, Laboratory for Stem Cell Translational Research, Kobe Institute of Biomedical Research and Innovation, 2–2 Minatojima-Minamimachi, Chuo-Ku, Kobe, 650–0047, Japan (e-mail asa777@aol.com); or Douglas W. Losordo, MD, Division of Cardiovascular Research, St Elizabeth's Medical Center, 736 Cambridge St, Boston, MA 02135 (e-mail douglas.losordo@tufts.edu).

Circulation is available at http://www.circulationaha.org

DOI: 10.1161/CIRCULATIONAHA.106.644518

tissue. The possibility for non-EPCs to differentiate into undesired lineage cells such as osteoblasts, chondroblasts, fibroblasts, adipocytes, or ectopic myocytes also remains to be clarified.

To the best of our knowledge, no report has compared the therapeutic potential and safety of EPC transplantation with those of tMNC administration. Accordingly, we performed transplantation of human EPCs compared with tMNCs in a model of rat myocardial infarction (MI) and investigated the effects of these 2 potential cellular therapies for ischemic neovascularization, inhibition of left ventricular (LV) remodeling, and preservation of LV function after acute MI.

Methods

These experiments were performed as a part of a pre-IND (investigational new drug) study, which supported a clinical trial of autologous $CD34^+$ cell transplantation in patients with coronary artery disease. Results of this study were submitted to the US Food and Drug Administration with the clinical protocol, which was approved in November 2003.

Cell Collection and Isolation

All procedures were approved by our institutional ethics committees. Peripheral blood tMNCs were obtained from 3 healthy volunteers who underwent leukoapheresis after subcutaneous administration of granulocyte colony-stimulating factor (5 $\mu g \cdot kg^{-1} \cdot d^{-1}$) for 5 days. We performed fluorescent-activated cell sorter analysis to examine the frequency of $CD34^+$ cells in the tMNCs. $CD34^+$ cells were isolated from tMNCs with the Isolex 300i $CD34^+$ cell isolation system (Baxter, Deerfield, Ill) as an EPC-enriched fraction. Fluorescent-activated cell sorter analysis revealed that the frequency of $CD34^+$ cells in the tMNCs was 1.7±0.9% and the purity of isolated $CD34^+$ cells was 90.1±8.1%.

Induction of Myocardial Ischemia and Cell Transplantation

All procedures were performed in accordance with the policies of our Institutional Animal Care and Use committees. Female athymic nude rats (Hsd:RH-rnu rats, Harlan Sprague Dawley, Indianapolis, Ind) 6 to 8 weeks of age were anesthetized with ketamine hydrochloride (75 mg/kg IP) and xylazine (10 mg/kg IP). Myocardial ischemia was induced by permanently ligating the left anterior descending (LAD) coronary artery under controlled ventilation.[4] Ten minutes after the LAD was ligated, 100 μL phosphate-buffered saline (PBS), 5×10^5 $CD34^+$ cells/kg, 5×10^5/kg of tMNCs (low-dose MNCs [loMNCs]), or a higher dose of tMNCs (hiMNCs) calculated to contain 5×10^5 $CD34^+$ cells/kg were injected intramyocardially into 5 sites in the ischemic LAD territory with a 27G needle (20 μL to each site) (n=9 to 11 in each group). All cells were suspended with 100 μL PBS. Cell number of the hiMNC group was determined from the results of the fluorescent-activated cell sorter analysis for CD34 described above. The ischemic zone was macroscopically identified by the pale color of the anterior and lateral walls immediately after LAD ligation.[6] Induction of myocardial ischemia and cell transplantation was performed by experienced researchers who were blinded to treatment assignment.

Histological Assessment of Transplanted Animals

Rats were anesthetized with ketamine hydrochloride and xylazine 3 days (n=6 to 8) and 28 days (n=8 to 11) after cell transplantation. Peripheral blood was obtained from the abdominal aorta of each rat for hematological examinations such as blood cell count, hemoglobin, and hematocrit and blood chemical examinations, including blood urea nitrogen, creatinine, alanine transaminase, aspartate transaminase, creatine kinase, lactic dehydrogenase, troponin I, and blood sugar. Immediately after blood collection, rats were killed with an overdose of ketamine hydrochloride. At necropsy, organs, comprising brain, lung, heart, liver, spleen, kidney, and ovary, from each animal were collected, weighed, and fixed with 4% paraformaldehyde. Hearts were also sliced in a bread-loaf fashion into 8 transverse sections from apex to base. In 3 additional rats in each group, heart samples collected on day 3 were similarly sliced, embedded in optimal cutting temperature compound, snap-frozen in liquid nitrogen, and stored at −80°C. Frozen heart samples were similarly obtained on day 28 in 5 additional rats in each group.

Paraffin-embedded tissues of all organs were stained with hematoxylin and eosin to histologically examine adverse events after cell transplantation. Severity of hemorrhagic infarction in ischemic myocardium on day 3 also was evaluated semiquantitatively using the hematoxylin and eosin–stained samples as follows: 0=none, 1=mild, 2=moderate, and 3=severe. Masson-trichrome staining was performed using the paraffin-embedded heart sections obtained 28 days after transplantation to measure the average ratio of fibrosis area to the entire LV area. Histochemical staining for the murine-specific endothelial cell marker isolectin B4 (Vector Laboratories, Burlingame, Calif)[4] was performed using the heart samples obtained 28 days after treatment. Capillary density was evaluated morphometrically by histological examination of 5 randomly selected fields of tissue sections recovered from segments of LV myocardium subserved by the occluded LAD. Capillaries were recognized as tubular structures positive for isolectin B4.

Frozen heart samples obtained on day 3 were used for immunohistochemistry with human-specific antibody against CD45 (BD Biosciences, San Jose, Calif) to identify hematopoietic/inflammatory cells derived from transplanted human cells in rat ischemic myocardium. Frozen samples on day 28 were used for immunohistochemistry with antibodies against human nuclear antigen (HNA), cardiac troponin I, and von Willebrand factor (vWF) (all from Chemicon International, Temecula, Calif) to detect cardiomyocytes and endothelial cells derived from transplanted human cells.

All morphometric studies were performed by 2 examiners who were blinded to treatment assignment.

Physiological Assessment of LV Function

Transthoracic echocardiography (SONOS 5500, Phillips Technologies, Bothell, Wash) was performed 28 days after transplantation. Fractional shortening was measured at the middle papillary muscle level. Regional wall motion score was examined per published criteria.[13] All procedures and analyses were performed by an experienced researcher who was blinded to treatment.

Statistical Analysis

Results were statistically analyzed with the use of the Statview 5.0 software package (Abacus Concepts Inc, Berkeley, Calif). Severity scores were examined across groups through the use of the Kruskal-Wallis test, followed by the Wilcoxon rank-sum test with the simple Bonferroni method (a value of $P<0.05/6$ was considered statistically significant). Intergroup comparison of incidence of moderate to severe hemorrhagic infarction on day 5 was assessed by χ^2 test (a value of $P<0.05$ was considered significant). Echocardiographic and histological values on day 28 were expressed as mean±SE. Scheffé's test was performed for the multiple comparisons after analysis of variance between groups. In Scheffé's test, a value of $P<0.05$ was considered statistically significant.

The authors had full access to the data and take responsibility for their integrity. All authors have read and agree to the manuscript as written.

Results

Exacerbation of Hemorrhagic MI Is Evident 3 Days After Transplantation of hiMNCs but Not loMNCs and Purified $CD34^+$ Cells

The weight of all organs was similar in all groups on days 3 and 28. Hematoxylin and eosin staining for all organs

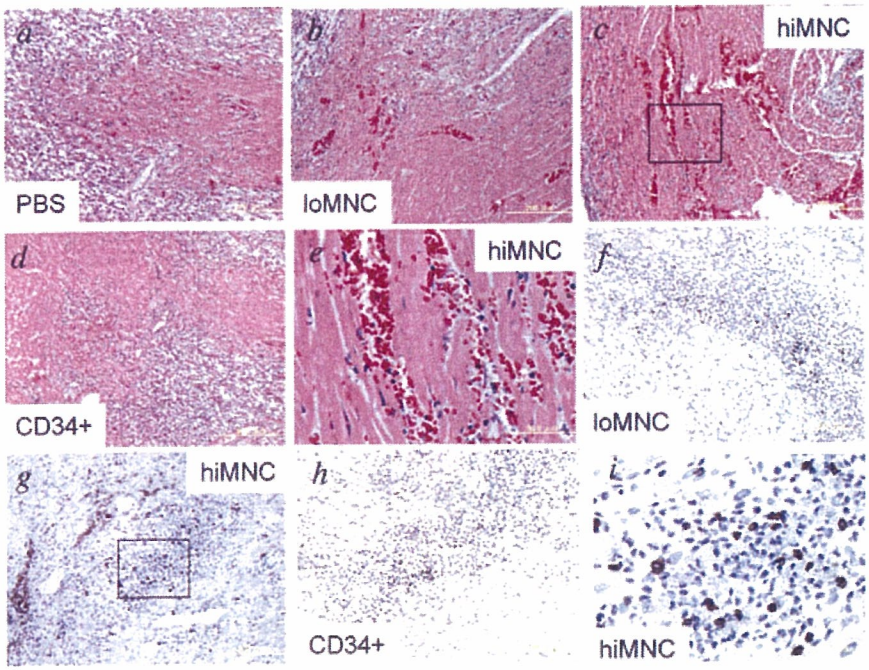

Figure 1. a–e, Representative light-microscope findings in infarcted myocardium 3 days after cell transplantation (hematoxylin and eosin staining; a–d, ×10; e, ×40). a, Rat receiving PBS; b, rat receiving 5×10^5 tMNC/kg (loMNC); c, e, rat receiving hiMNCs containing 5×10^5 $CD34^+$ cells/kg; d, rat receiving 5×10^5 $CD34^+$ cells/kg ($CD34^+$). f–i, Representative findings of immunohistochemistry for human-specific CD45 (f–h, ×10; i, ×40). Abundant distribution of human $CD45^+$ cells was observed in the hiMNC group (g and i) but not in the loMNC (f) and $CD34^+$ cell (h) groups.

except the heart disclosed no abnormal findings on days 3 and 28. Results of hematologic and blood chemical tests were similar in all groups on days 3 and 28 (data not shown).

Hematoxylin and eosin staining of myocardial tissue samples on day 3 revealed that the frequency of moderate to severe hemorrhagic MI was significantly greater in rats receiving hiMNCs compared with the PBS and $CD34^+$ cell groups (hiMNC, 87.5%, n=8; PBS, 33.3%, n=6; $CD34^+$, 12.5%, n=8; $P=0.04$ versus PBS and $P=0.003$ versus $CD34^+$ cell group). Frequency of severe hemorrhagic MI also was greater in the hiMNC group than in the $CD34^+$ cell group (hiMNC, 50.0%; $CD34^+$ cell, 0.0%; $P=0.02$). The severity score of hemorrhagic MI had a tendency to be greater in the hiMNC group (50.0% severe, 37.5% moderate, 12.5% mild, and 0.0% none) than in the PBS group (16.7% severe, 16.7% moderate, 50.0% mild, and 16.7% none) and $CD34^+$ cell group (0.0% severe, 12.5% moderate, 75.0% mild, and 12.5% none); however, these differences were not statistically significant ($P=0.04$ versus PBS, $P=0.01$ versus $CD34^+$) because a value of $P<0.05/6$ was considered significant by Bonferroni's method. The severity of hemorrhagic infarction was similar in the PBS, loMNC (28.6% severe, 28.6% moderate, 28.6% mild, and 14.3% none; n=7), and $CD34^+$ cell groups (Figure 1a through 1e).

Immunohistochemistry for human-specific CD45 revealed more abundant distribution of human $CD45^+$ cells within the ischemic myocardium of the hiMNC group compared with the $CD34^+$ cell and loMNC groups. The human $CD45^+$ cells were mainly round without a tubular structure, a finding that strongly suggests differentiation of transplanted human cells into hematopoietic/inflammatory cells in the rat ischemic myocardium. Human-specific $CD45^+$ cells were not observed in the PBS group (Figure 1f through 1i).

These results suggest that transplantation of unselected human MNCs may worsen hemorrhagic MI, perhaps via distribution of hematopoietic/inflammatory cells into the acutely ischemic myocardium. This unfavorable phenomenon was not observed after transplantation of loMNCs and $CD34^+$ cells.

Transplanted $CD34^+$ Cells Differentiate More Abundantly Into Cardiomyocytes and Endothelial Cells in the Infarcted Myocardium on Day 28 Compared With Unpurified tMNCs

Double immunostainings for HNA and cardiac troponin I to detect transplanted human cell–derived cardiomyocytes and for HNA and vWF to identify human cell–derived endothelial cells were performed using samples of the infarcted myocardium at day 28. These stainings revealed that double-positive cells for HNA and cardiac troponin I were identified only in rats receiving $CD34^+$ cells but not in the hiMNC, loMNC, and PBS groups (Figure 2a through 2h). Similarly, double-positive cells for HNA and vWF were abundant in the $CD34^+$ cell group and rare in the hiMNC group. The double-positive cells were not observed in the loMNC and PBS groups (Figure 2i through 2p).

These results suggest that purified $CD34^+$ cell transplantation may have more potential for cardiac myoangiogenesis compared with total MNC transfer.

Transplantation of $CD34^+$ Cells Further Augments Ischemic Neovascularization and Inhibits LV Remodeling on Day 28 Compared With That of Unpurified tMNCs

Capillary density 28 days after treatment was significantly greater in the $CD34^+$ cell group (721.1 ± 19.9 per 1 mm^2) than in the PBS, loMNC, and hiMNC groups (384.7 ± 11.0, 372.5 ± 14.1, and 497.5 ± 24.0 per 1 mm^2, respectively)

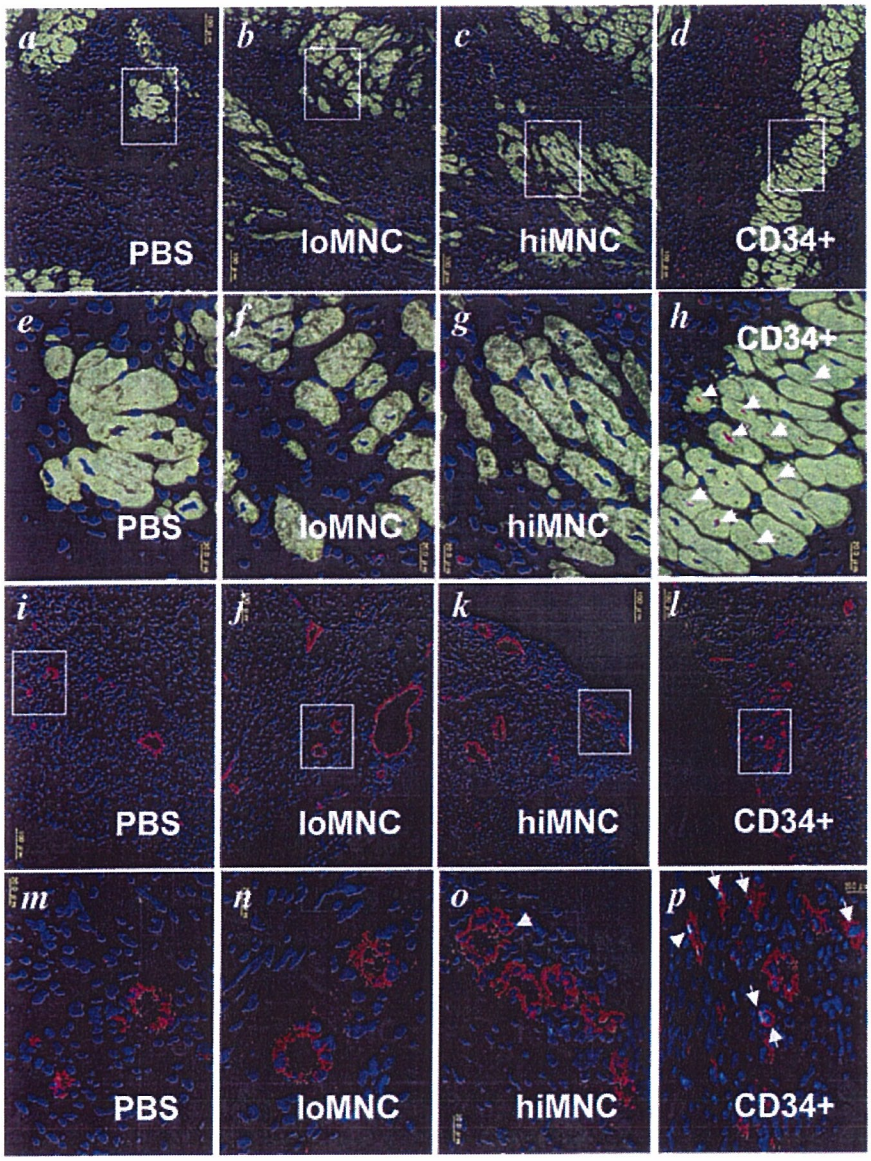

Figure 2. a–h, Representative double immunohistochemistry for HNA (red) and cardiac troponin I (green) in PBS (a, e), loMNC (b, f), hiMNC (c, g), and $CD34^+$ cell (d, h) groups. Blue fluorescence demonstrates 4′6-diamidino-2-phenylindole (DAPI) for nuclear staining. a–d, ×10; e–h, ×40; arrows indicate nuclei of cardiomyocytes expressing HNA (purple, double positive for HNA and DAPI), which indicates differentiation of transplanted human cells into cardiomyocytes. The cardiomyogenic differentiation was identified only in the $CD34^+$ cell group. i–p, Representative double immunostaining for HNA (green) and vWF (red) in the PBS (i, m), loMNC (j, n), hiMNC (k, o), and $CD34^+$ cell (l, p) groups. Blue fluorescence demonstrates DAPI for nuclear staining. i–l, ×10; m–p, ×40; arrows show nuclei of endothelial cells expressing HNA (pale green, double positive for HNA and DAPI), which indicates differentiation of transplanted human cells into endothelial cells. The vasculogenic differentiation was abundantly detected in the $CD34^+$ cell group and rarely in the hiMNC group but not in the loMNC and PBS groups.

($P<0.0001$ versus PBS, loMNC, and hiMNC groups). Capillary density on day 28 also was significantly greater in the hiMNC group than in the PBS and loMNC groups ($P=0.003$ versus PBS group, $P=0.001$ versus loMNC group). Capillary density on day 28 in the loMNC group was not significantly different from that in the PBS group (Figure 3a through 3e).

The ratio of percent fibrosis area to entire LV area was significantly lower in the $CD34^+$ cell group ($15.6\pm0.9\%$) than in the PBS, loMNC, and hiMNC groups ($26.3\pm1.2\%$, $27.5\pm1.8\%$, and $22.2\pm1.8\%$, respectively) ($P=0.0003$ versus PBS group, $P<0.0001$ versus loMNC group, $P=0.02$ versus hiMNC group). This ratio was similar between the PBS, loMNC, and hiMNC groups (Figure 3f through 3j).

Thus, transplantation of hiMNCs significantly augmented ischemic neovascularization; however, transplantation of $CD34^+$ cells enhanced new blood vessel formation to a greater degree than when the same dose of $CD34^+$ cells was administered within an unselected MNC population. Furthermore, only transplantation of $CD34^+$ cells significantly inhibited LV remodeling after MI.

Transplantation of $CD34^+$ Cells Preserves LV Function After Myocardial Ischemia

By day 28 after treatment, fractional shortening was significantly higher in the $CD34^+$ cell group ($30.3\pm0.9\%$) than in the PBS, loMNC, and hiMNC groups ($22.7\pm1.5\%$, $23.4\pm1.1\%$, and $24.9\pm1.7\%$, respectively) ($P=0.007$ versus PBS, $P=0.02$ versus loMNC, $P=0.049$ versus hiMNC group). Fractional shortening on day 28 was similar in the PBS, loMNC, and hiMNC groups (Figure 4a and 4b). Regional wall motion score was better preserved in the $CD34^+$ cell group (21.8 ± 0.5) than in the PBS, loMNC, and hiMNC groups (25.4 ± 0.4, 24.9 ± 0.4, and 24.1 ± 0.6, respectively) ($P=0.0004$ versus PBS, $P=0.002$ versus loMNC, $P=0.02$ versus hiMNC group). Regional wall motion score was similar in the PBS, loMNC, and hiMNC groups (Figure 4a and 4c).

Thus, echocardiographic examination performed in the chronic phase after MI suggests that transplantation of

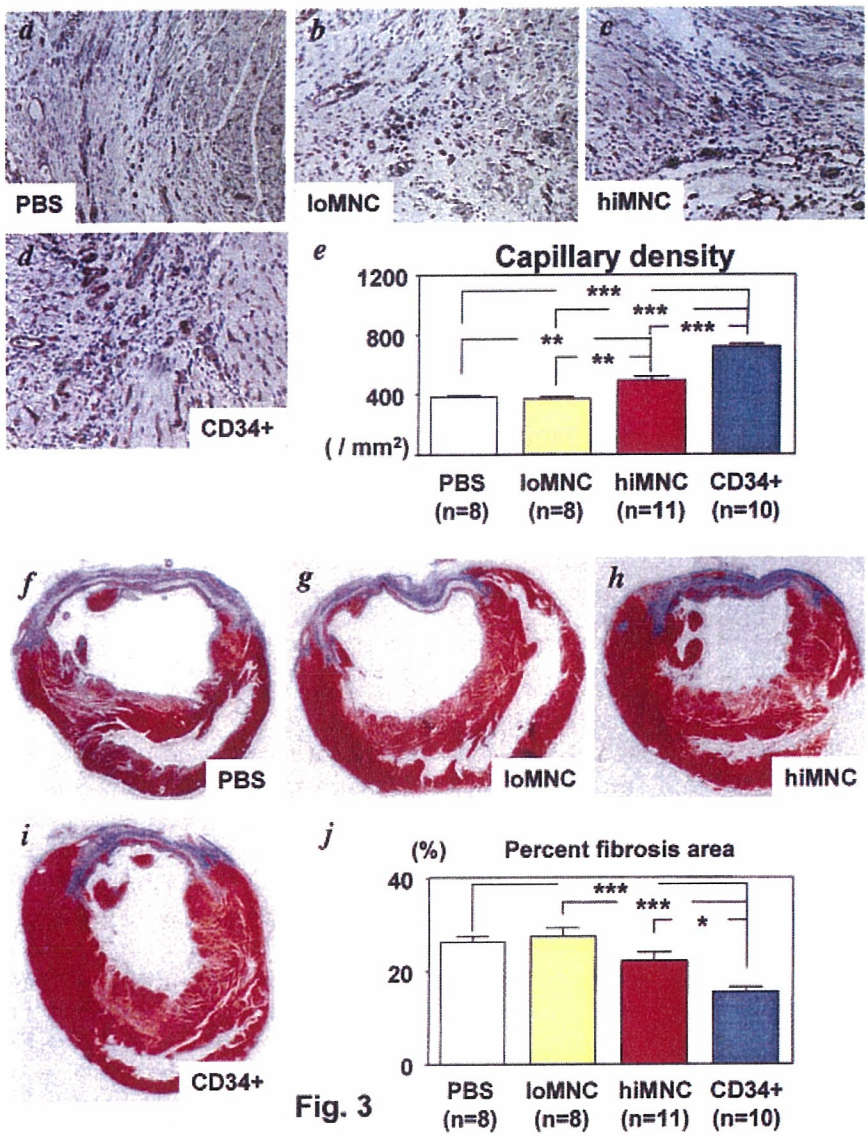

Fig. 3

Figure 3. a–d, Representative findings of histochemical staining for isolectin B4 in the ischemic myocardium 4 weeks after treatment (×20). a, Rat receiving PBS; b, rat receiving loMNCs; c, rat receiving hiMNCs; d, rat receiving 5×10^5 $CD34^+$ cells/kg ($CD34^+$). e, Capillary density in ischemic myocardium 4 weeks after each treatment. f–i, Representative findings of elastic tissue trichrome staining in heart samples 4 weeks after MI. These samples were obtained from rats receiving PBS (f), loMNCs (g), hiMNCs (h), and $CD34^+$ cells (i). j, Ratio of fibrosis area to entire LV area (percent fibrosis area) 4 weeks after each treatment. $^*P<0.05$; $^{**}P<0.01$; $^{***}P<0.001$.

$CD34^+$ cells may have a favorable impact on the preservation of global and regional LV function. Transplantation of higher doses of unselected tMNCs also had a tendency to preserve LV contractility after MI, but this change was not significant.

Discussion

In the present study, dosages of $CD34^+$ cells and tMNCs were determined on the basis of our previous animal study in anticipation of a future clinical trial. In the previous study[6] evaluating intramyocardial transplantation of $CD34^+$ cells into rats with MI, the effective cell dose for ischemic neovascularization and preservation of LV function was 10^5 cells per rat, which is equivalent to 5 to 7×10^5 cells/kg. Previous clinical reports in the hematology field indicated that the estimated number of autologous $CD34^+$ cells obtained by single leukoapheresis after a 5-day administration of granulocyte colony-stimulating factor is 5 to 10×10^5 cells/kg.[14,15] Therefore, we anticipated that transfer of 5×10^5 $CD34^+$ cells/kg would be both an effective and a clinically realistic dose. To precisely assess the difference of safety and therapeutic potential between purified $CD34^+$ cells and tMNCs, we also included 2 treatment groups of tMNCs: the same total dose of tMNCs (loMNC) as the $CD34^+$ cells (5×10^5 cells/kg) and high-dose tMNCs (hiMNC) containing an equivalent dose of $CD34^+$ cells (5×10^5 $CD34^+$ cells/kg).

Histological findings in the acute phase of MI (on day 3) revealed that the incidence of moderate to severe hemorrhagic infarction, which is one of the prognostic signs of irreversible myocardial and microvascular damage after MI,[16,17] was significantly greater after hiMNC transplantation than PBS or $CD34^+$ cell injection. This unfavorable phenomenon was not observed in the loMNC group. These findings suggest that intramyocardial transplantation of tMNCs into acutely ischemic myocardium may be safe up to 5×10^5 cells/kg but may worsen hemorrhagic infarction at higher doses (10^7 cells/kg). The present findings also indicate that the hemorrhagic issue is not present in the case of $CD34^+$ cell transplantation at a dose of up to 5×10^5 cells/kg. The exact mechanism of hemorrhagic infarction in the hiMNC group is unknown; however, immunohisto-

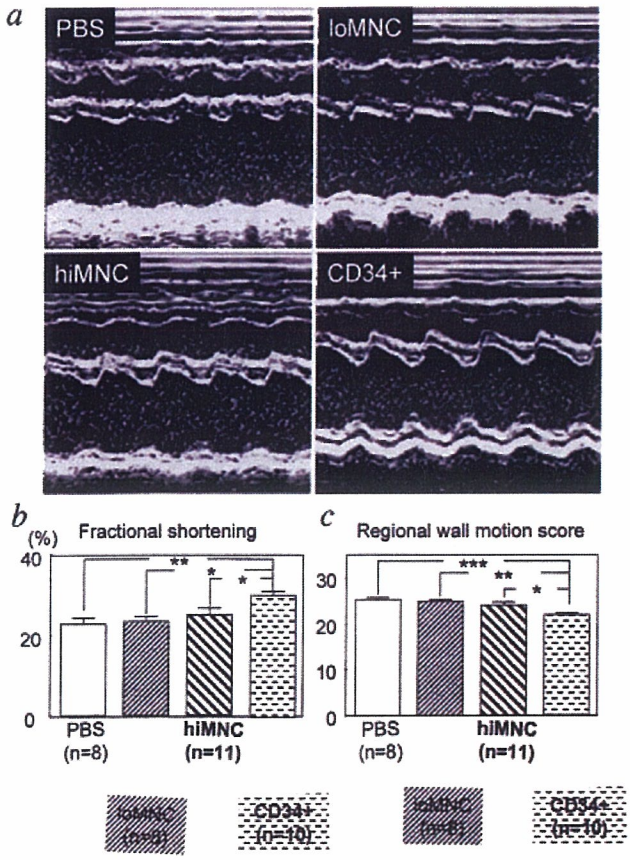

Figure 4. a, Representative M-mode echocardiography 4 weeks after each treatment. b, c, Echocardiographic fractional shortening (b) and regional wall motion score (c) in all treatment groups 4 weeks after MI. $^{*}P<0.05$; $^{**}P<0.01$, $^{***}P<0.001$.

chemical evidence of abundant human-specific $CD45^+$ cells in rat ischemic myocardium suggests that higher numbers of hematopoietic/inflammatory cells derived from transplanted human cells may play a key role in accelerating myocardial damage after MI in the hiMNC group. Recently, we have reported differentiation of transplanted human $CD34^+$ cells into cardiomyocytes and endothelial cells in infarcted myocardium of nude rats at day 28.[18] The favorable effects of $CD34^+$ cells were proved not only by immunohistochemistry but also by a molecular approach including fluorescent in situ hybridization. In the present study, a similar regenerative property at the chronic phase was immunohistochemically confirmed in the $CD34^+$ cell group but not in the tMNC and PBS groups. The detailed mechanism of the different outcome in each group is unclear; however, loMNCs contain fewer $CD34^+$ cells, which are beneficial for cardiomyogenesis. In the case of hiMNC transplantation, severe hemorrhage/inflammation in the acute phase may be harmful for survival and differentiation of the transplanted cells in the chronic phase. These results indicate that purified $CD34^+$ cell transplantation may have more potential for cardiac myoangiogenesis in the chronic phase of MI compared with total MNC transfer.

Regarding therapeutic potential of the cell therapy after MI, morphometric analyses revealed superiority of $CD34^+$ cell transplantation to tMNC administration. Capillary density in the ischemic myocardium was significantly greater in the hiMNC group than in the PBS and loMNC groups but was superior in the $CD34^+$ cell group compared with the hiMNC group. LV remodeling evaluated by percent fibrosis area also was significantly reduced in the $CD34^+$ cell group compared with all other groups. Percent fibrosis area in the hiMNC group was similar to that in the PBS and loMNC groups despite significant augmentation of ischemic neovascularization. Echocardiographic examinations also demonstrated significantly better outcomes in terms of preservation of both global and regional LV function only in the $CD34^+$ cell group, not in the loMNC and hiMNC groups. These findings suggest that purified $CD34^+$ cells may have more potency for preservation/recovery of LV structural integrity and function in the chronic phase after MI. Taken together with the results in the acute phase after MI, $CD34^+$ cell transplantation may exhibit increased potency and safety in both the acute and chronic phases after MI for therapeutic neovascularization compared with tMNCs. Transplantation of loMNCs may not have significant efficacy for the histological and physiological recovery from MI in the chronic phase despite safety during the acute phase. Moreover, administration of hiMNCs may not achieve a therapeutic effect in the chronic phase equivalent to that of purified $CD34^+$ cells despite equal dosing of $CD34^+$ cells. The diminished effect of hiMNCs in the chronic phase may relate to increased myocardial damage during the acute phase.

A recent clinical report[19] demonstrated that purified $CD34^+$ cells incorporate more efficiently into the ischemic border-zone myocardium after intracoronary infusion compared with unselected tMNCs. In addition to the recent report in the case of intracoronary cell infusion, the present study may provide important information regarding the superiority of $CD34^+$ cells over tMNCs in terms of safety and efficacy after intramyocardial cell transfer.

The present findings provide additional data supporting the selection of specific cell types for applications in myocardial repair after ischemic injury and serve, along with abundant safety data, as the scientific underpinnings for a human pilot clinical trial. These data underscore one of the advantages of cell-based therapies: the ability to actually test the potency of the proposed therapeutic, ie, the human cells themselves. Existing data have documented the varying potency of cells collected from patients with vascular disease and cardiac risk factors.[20] Our findings suggest that within the population of circulating cells, subsets exist that may be safer and more potent for myocardial repair. Further mechanistic data identifying the phenotypic features that define potency will move the field of cell therapy forward.

Acknowledgments

We thank Dr Satoshi Teramukai (Translational Research Informatics, Kobe, Japan) for his statistical advice and Mickey Neely for her secretarial assistance.

Sources of Funding

This study was supported in part by National Institutes of Health grants (HL-53354, HL-57516, HL-63414, HL-77428, HL-80137, and HLP01-66957) and Health and Labor Sciences research grants (H17-trans-002) from the Japanese Ministry of Health, Labor, and Welfare.

Disclosure

Dr Losordo has significant relationships as a principal investigator, collaborator, or consultant on research grants with the following companies: Baxter, Inc, Corautus, Cordis, Curis, Anormed, and Boston Scientific Corp.

References

1. Asahara T, Murohara T, Sullivan A, Silver M, van der Zee R, Li T, Witzenbichler B, Schatteman G, Isner JM. Isolation of putative progenitor endothelial cells for angiogenesis. *Science*. 1997;275:964–967.
2. Kalka C, Masuda H, Takahashi T, Kalka-Moll WM, Silver M, Kearney M, Li T, Isner JM, Asahara T. Transplantation of ex vivo expanded endothelial progenitor cells for therapeutic neovascularization. *Proc Natl Acad Sci U S A*. 2000;97:3422–3427.
3. Murohara T. Therapeutic vasculogenesis using human cord blood-derived endothelial progenitors. *Trends Cardiovasc Med*. 2001;11:303–307.
4. Kawamoto A, Gwon HC, Iwaguro H, Yamaguchi JI, Uchida S, Masuda H, Silver M, Ma H, Kearney M, Isner JM, Asahara T. Therapeutic potential of ex vivo expanded endothelial progenitor cells for myocardial ischemia. *Circulation*. 2001;103:634–637.
5. Kocher AA, Schuster MD, Szabolcs MJ, Takuma S, Burkhoff D, Wang J, Homma S, Edwards NM, Itescu S. Neovascularization of ischemic myocardium by human bone-marrow-derived angioblasts prevents cardiomyocyte apoptosis, reduces remodeling and improves cardiac function. *Nat Med*. 2001;7:430–436.
6. Kawamoto A, Tkebuchava T, Yamaguchi J, Nishimura H, Yoon YS, Milliken C, Uchida S, Masuo O, Iwaguro H, Ma H, Hanley A, Silver M, Kearney M, Losordo DW, Isner JM, Asahara T. Intramyocardial transplantation of autologous endothelial progenitor cells for therapeutic neovascularization of myocardial ischemia. *Circulation*. 2003;107:461–468.
7. Assmus B, Schachinger V, Teupe C, Britten M, Lehmann R, Dobert N, Grunwald F, Aicher A, Urbich C, Martin H, Hoelzer D, Dimmeler S, Zeiher AM. Transplantation of Progenitor Cells and Regeneration Enhancement in Acute Myocardial Infarction (TOPCARE-AMI). *Circulation*. 2002;106:3009–3017.
8. Stamm C, Westphal B, Kleine HD, Petzsch M, Kittner C, Klinge H, Schumichen C, Nienaber CA, Freund M, Steinhoff G. Autologous bone-marrow stem-cell transplantation for myocardial regeneration. *Lancet*. 2003;361:45–46.
9. Fuchs S, Baffour R, Zhou YF, Shou M, Pierre A, Tio FO, Weissman NJ, Leon MB, Epstein SE, Kornowski R. Transendocardial delivery of autologous bone marrow enhances collateral perfusion and regional function in pigs with chronic experimental myocardial ischemia. *J Am Coll Cardiol*. 2001;37:1726–1732.
10. Kamihata H, Matsubara H, Nishiue T, Fujiyama S, Tsutsumi Y, Ozono R, Masaki H, Mori Y, Iba O, Tateishi E, Kosaki A, Shintani S, Murohara T, Imaizumi T, Iwasaka T. Implantation of bone marrow mononuclear cells into ischemic myocardium enhances collateral perfusion and regional function via side supply of angioblasts, angiogenic ligands, and cytokines. *Circulation*. 2001;104:1046–1052.
11. Tateishi-Yuyama E, Matsubara H, Murohara T, Ikeda U, Shintani S, Masaki H, Amano K, Kishimoto Y, Yoshimoto K, Akashi H, Shimada K, Iwasaka T, Imaizumi T. Therapeutic angiogenesis for patients with limb ischaemia by autologous transplantation of bone-marrow cells: a pilot study and a randomised controlled trial. *Lancet*. 2002;360:427–435.
12. Perin EC, Dohmann HF, Borojevic R, Silva SA, Sousa AL, Mesquita CT, Rossi MI, Carvalho AC, Dutra HS, Dohmann HJ, Silva GV, Belem L, Vivacqua R, Rangel FO, Esporcatte R, Geng YJ, Vaughn WK, Assad JA, Mesquita ET, Willerson JT. Transendocardial, autologous bone marrow cell transplantation for severe, chronic ischemic heart failure. *Circulation*. 2003;107:2294–2302.
13. Schiller NB, Shah PM, Crawford M, DeMaria A, Devereux R, Feigenbaum H, Gutgesell H, Reichek N, Sahn D, Schnittger I. Recommendations for quantitation of the left ventricle by two-dimensional echocardiography: American Society of Echocardiography Committee on Standards, Subcommittee on Quantitation of Two-Dimensional Echocardiograms. *J Am Soc Echocardiogr*. 1989;2:358–367.
14. Grigg AP, Roberts AW, Raunow H, Houghton S, Layton JE, Boyd AW, McGrath KM, Maher D. Optimizing dose and scheduling of filgrastim (granulocyte colony-stimulating factor) for mobilization and collection of peripheral blood progenitor cells in normal volunteers. *Blood*. 1995;86:4437–4445.
15. Martinez C, Urbano-Ispizua A, Rozman C, Marin P, Mazzara R, Carreras E, Rovira M, Sierra J, Briones J, Ordinas A, Montserrat E. Effects of G-CSF administration and peripheral blood progenitor cell collection in 20 healthy donors. *Ann Hematol*. 1996;72:269–272.
16. Pislaru SV, Barrios L, Stassen T, Jun L, Pislaru C, Van de Werf F. Infarct size, myocardial hemorrhage, and recovery of function after mechanical versus pharmacological reperfusion: effects of lytic state and occlusion time. *Circulation*. 1997;96:659–666.
17. Asanuma T, Tanabe K, Ochiai K, Yoshitomi H, Nakamura K, Murakami Y, Sano K, Shimada T, Murakami R, Morioka S, Beppu S. Relationship between progressive microvascular damage and intramyocardial hemorrhage in patients with reperfused anterior myocardial infarction: myocardial contrast echocardiographic study. *Circulation*. 1997;96:448–453.
18. Iwasaki H, Kawamoto A, Ishikawa M, Oyamada A, Nakamori S, Nishimura H, Sadamoto K, Horii M, Matsumoto T, Murasawa S, Shibata T, Suehiro S, Asahara T. Dose-dependent contribution of CD34-positive cell transplantation to concurrent vasculogenesis and cardiomyogenesis for functional regenerative recovery after myocardial infarction. *Circulation*. 2006;113:1311–1325.
19. Hofmann M, Wollert KC, Meyer GP, Menke A, Arseniev L, Hertenstein B, Ganser A, Knapp WH, Drexler H. Monitoring of bone marrow cell homing into the infarcted human myocardium. *Circulation*. 2005;111:2198–2202.
20. Vasa M, Fichtlscherer S, Aicher A, Adler K, Urbich C, Martin H, Zeiher AM, Dimmeler S. Number and migratory activity of circulating endothelial progenitor cells inversely correlate with risk factors for coronary artery disease. *Circ Res*. 2001;89:E1–E7.

CLINICAL PERSPECTIVE

These preclinical studies provide evidence for increased safety and potency of CD34+ cell therapy for treatment of myocardial ischemia and form the basis for a recently completed phase 1/2 clinical trial. The selection of CD34+ cells was originally performed in the setting of stem cell transplantation for reconstitution of hematopoiesis; however, it became apparent that in many settings the unselected mononuclear cell population also was capable of achieving this goal, and the selection procedure was largely abandoned in that context. The present studies were designed to determine whether this was also the case when the CD34+ stem cell was used for neovascularization of ischemic tissue. The data reveal that all parameters of safety and efficacy are significantly improved after intramyocardial transplantation of CD34+ cells compared with treatment with an equal dose (cell number) of unselected mononuclear cells. The same was true when the mononuclear cell dose was adjusted to achieve an equivalent dose of CD34+ cells, suggesting that the unselected cells contain elements that impair the salutary effects of CD34+ cells on myocardial repair. These data provide further evidence that the CD34+ cell is a suitable platform for cell-based ischemic tissue repair and that selected cells offer a safety and potency advantage.

The American Journal of Pathology, Vol. 169, No. 4, October 2006

DOI: 10.2353/ajpath.2006.060064

Vascular Biology, Atherosclerosis and Endothelium Biology

Therapeutic Potential of Vasculogenesis and Osteogenesis Promoted by Peripheral Blood CD34-Positive Cells for Functional Bone Healing

Tomoyuki Matsumoto,*† Atsuhiko Kawamoto,* Ryosuke Kuroda,† Masakazu Ishikawa,* Yutaka Mifune,*† Hiroto Iwasaki,* Masahiko Miwa,† Miki Horii,* Saeko Hayashi,* Akira Oyamada,* Hiromi Nishimura,* Satoshi Murasawa,* Minoru Doita,† Masahiro Kurosaka,† and Takayuki Asahara*‡

From Stem Cell Translational Research, Kobe Institute of Biomedical Research and Innovation/Riken Center for Developmental Biology, Kobe; the Department of Orthopedic Surgery,† Kobe University Graduate School of Medicine, Kobe; and the Department of Regenerative Medicine Science,‡ Tokai University School of Medicine, Tokai, Japan*

Failures in fracture healing are mainly caused by a lack of vascularization. Adult human circulating $CD34^+$ cells, an endothelial/hematopoietic progenitor-enriched cell population, have been reported to differentiate into osteoblasts *in vitro*; however, the therapeutic potential of $CD34^+$ cells for fracture healing is still unclear. Therefore, we performed a series of experiments to test our hypothesis that functional fracture healing is supported by vasculogenesis and osteogenesis via regenerative plasticity of $CD34^+$ cells. Peripheral blood $CD34^+$ cells, isolated from total mononuclear cells of adult human volunteers, showed gene expression of osteocalcin in 4 of 20 freshly isolated cells by single cell reverse transcriptase-polymerase chain reaction analysis. Phosphate-buffered saline, mononuclear cells, or $CD34^+$ cells were intravenously transplanted after producing nonhealing femoral fractures in nude rats. Reverse transcriptase-polymerase chain reaction and immunohistochemical staining at the peri-fracture site demonstrated molecular and histological expression of human-specific markers for endothelial cells and osteoblasts at week 2. Functional bone healing assessed by biomechanical as well as radiological and histological examinations was significantly enhanced by $CD34^+$ cell transplantation compared with the other groups. Our data suggest circulating human $CD34^+$ cells have therapeutic potential to promote an environment conducive to neovascularization and osteogenesis in damaged skeletal tissue, allowing the complete healing of fractures. ***(Am J Pathol 2006, 169:1440–1457; DOI: 10.2353/ajpath.2006.060064)***

Whereas embryonic stem cells in the blastocyst stage have the ability to generate any differentiated cells in the body, most adult stem cells have limited potential for postnatal tissue/organ regeneration. Among phenotypically characterized adult stem/progenitor cells,[1–3] the hematopoietic system has traditionally been considered as an organized, hierarchic system with multipotent, self-renewing stem cells at the top, lineage-committed progenitor cells in the middle, and lineage-restricted precursor cells, which give rise to terminally differentiated cells, at the bottom.[4] Recently, adult human peripheral blood $CD34^+$ cells have been reported to contain intensive endothelial progenitor cells (EPCs) as well as hematopoietic stem cells (HSCs).[5] Tissue ischemia and cytokines mobilize EPCs from bone marrow (BM) into peripheral blood, and mobilized EPCs specifically home to sites of nascent neovascularization and differentiate into mature endothelial cells (ECs) (vasculogenesis).[6,7] In the case of the immunodeficient rat model of acute myocardial infarction, transplanted human $CD34^+$ cells or *ex vivo* expanded EPCs incorporate into the site of the myocardial neovascularization, differentiate into mature ECs, augment capillary density, inhibit myocardial fibrosis and apoptosis, and preserve the left ventricular function.[8–10] In addition, intravenously transplanted $CD34^+$ cells efficiently incorporate into ischemic tissue.[9,11]

In recent years, in an attempt to meet clinical demands, interest has turned to bone formation as an alternative category of regenerative medicine. It is anticipated that by optimizing the process of fracture repair, a biological approach results in the restoration of normal struc-

Accepted for publication June 20, 2006.

Address reprint requests to Takayuki Asahara, M.D., Stem Cell Translational Research, Kobe Institute of Biomedical Research and Innovation/Riken Center for Developmental Biology, 2-2 Minatojima-Minamimachi, Chuo-ku, Kobe 650-0047. E-mail: asa777@aol.com.

ture and function in the injured skeletal tissue. Although most fractures typically heal with callus formation that bridges the fracture gap, a significant proportion (5 to 10%) of fractures fail to heal and result in delayed union or persistent nonunion.[12,13] Inappropriate neoangiogenesis is considered to be a crucial factor in failed bone formation and remodeling.[14,15] Notably, appropriate vascularization is emerging as a prerequisite for bone development and regeneration, and indeed there appears to be a developmental reciprocity between ECs and osteoblasts (OBs).[16] Under such recognition, human CD34$^+$ cells, which are capable of generating ECs in an appropriate environment,[6,7] have also been reported to differentiate into OBs *in vitro*.[17–19] In addition, a recent report demonstrated that CD34$^+$ osteoblastic cells line the cavities of the cartilage in the fracture site in a rabbit tibial osteotomy model.[20] These observations provoked the hypothesis that human peripheral blood CD34$^+$ cells play a key role in fracture healing via vasculogenesis and osteogenesis. Therefore, we first confirmed that mouse Scal$^-$ lineage marker$^-$ (Lin$^-$) cells, quite similar to human CD34$^+$ cells,[7,21,22] were mobilized to peripheral blood in the natural course of the fracture healing process. Next, we investigated whether transplantation of circulating human CD34$^+$ cells contributed to both vasculogenesis and osteogenesis for functional bone healing after fracture in an immunodeficient rat model.

In the present series of studies, we demonstrate that mouse Scal$^+$Lin$^-$ cells are mobilized into the peripheral blood in the natural course of fracture healing and that human peripheral blood CD34$^+$ cells, containing osteo/endothelial progenitor cells already expressing osteocalcin (OC), which were recruited to the fracture site after systemic delivery, develop a favorable environment for fracture healing by enhancing vasculogenesis and osteogenesis and finally lead to functional recovery from fracture. The present findings have important clinical implications for cell-based therapy that will enhance bone repair after fracture.

Materials and Methods

Isolation of Mouse Lin$^-$ Cells and Assessment of Scal$^+$Lin$^-$ Cells

To confirm the kinetics of Scal$^+$Lin$^-$ cells in the natural course of fracture healing, we detected Scal$^+$Lin$^-$ cells at prefracture and 1, 4, 7, and 14 days after fracture by fluorescence-activated cell sorting (FACS) analysis (n = 3 in each). Peripheral blood cells were aspirated from the hearts of 10-week-old fractured mice 1, 4, 7, and 14 days after fracture and from those of unfractured mice and mixed with phosphate-buffered saline (PBS) containing 5% fetal calf serum (n = 3 in each). MNCs were obtained by a Histopaque-1083 (Sigma Co., St. Louis, MO) density gradient centrifugation at 400 × g for 20 minutes. The light-density MNCs were collected, washed twice with Dulbecco's PBS supplemented with 2 mmol/L ethylenediaminetetraacetic acid, and counted manually. Separation of Lin$^-$ cells was performed to deplete mature hematopoietic cells[7,21] such as T cells, B cells, natural killer (NK) cells, monocytes/macrophages, granulocytes, and erythrocytes by labeling MNCs with a Lin$^-$ separation kit (BD Pharmingen, San Diego, CA), containing biotin-conjugated Mac1, B220, CD3e, Ter119, Ly6G, and CD45R antibodies followed by streptavidin-conjugated magnetic beads and BD IMagnet separation. Then, Lin$^-$ MNCs were counted, and the number of Scal$^+$Lin$^-$ cells was calculated from the rate of Scal$^+$ cells in Lin$^-$ MNCs by FACS analysis and the number of Lin$^-$ MNCs.

Isolation of CD34$^+$ Cells from Adult Human Volunteers

Human peripheral blood total MNCs were obtained from healthy male volunteers age 31.7 ± 1.2 years (n = 3). CD34$^+$ cells were isolated from the MNCs by the AutoMACS system (Miltenyi Biotec, Auburn, CA) using anti-CD34 microbeads (Miltenyi Biotec). The CD34$^+$ cell fraction had a purity of >97%, as determined by FACS analysis using a CD34-specific monoclonal antibody (Becton Dickinson, San Jose, CA). Institutional review board approval for the collection of peripheral blood MNCs from healthy human volunteers and informed consent regarding the experimental use of the cells from the volunteers were obtained.

Flow Cytometry Studies and Monoclonal Antibodies

Regular flow cytometric profiles were analyzed with a FACS Calibur analyzer and CELLQuest software (Becton Dickinson Immunocytometry Systems, Mountain View, CA). The instrument was aligned and calibrated daily using a four-color mixture of CaliBRITE beads (BD Biosciences) with FACSComp software (BD Bioscience). Dead cells were excluded from the plots' beads on propidium iodide (PI) staining (Sigma Co.). Human CD34$^+$ cells or mouse Lin$^-$ cells were washed twice with Hanks' balanced salt solution containing 3.0% fetal calf serum, incubated with 10 μl of FcR blocking reagent to increase the specificity of monoclonal antibodies (Miltenyi Biotec) for 20 minutes at 4°C, and incubated with the monoclonal antibodies for 30 minutes at 4°C. The stained cells were washed three times with PBS containing 3.0% fetal calf serum, resuspended in 0.5 ml of Hanks' balanced salt solution/3% fetal calf serum/propidium iodide, and analyzed by FACScan Caliber flow cytometer (Becton-Dickinson, Franklin Lakes, NJ). Cells (1×10^6) were processed through the cytometer, and 3×10^4 cells per sample were analyzed for human CD34$^+$ cell or mouse Lin$^-$ cell fraction. The following monoclonal anti-human antibodies were used to characterize the CD34$^+$ cell population: CD34-APC (BD Pharmingen), CD34-FITC (BD Pharmingen), CD45-FITC (BD Pharmingen), CD133-APC (BD Pharmingen), c-Kit-FITC (Nichirei), CD31-FITC (BD Pharmingen), CD105 (BD Pharmingen), VE cadherin (VE-cad)-FITC (BD Pharmingen), KDR-PE (BD Pharmingen), Tie2-PE (BD Pharmingen), IgG1-FITC isotype con-

trols (BD Pharmingen), IgG1-APC isotype controls (BD Pharmingen), and propidium iodide (Sigma Co.). The following monoclonal anti-mouse antibodies were used to characterize the Lin^- MNCs: cKit-APC (BD Pharmingen), Scal-FITC (BD Pharmingen), IgG2a-PE isotype controls (BD Pharmingen), IgG2a-FITC isotype controls (BD Pharmingen), and propidium iodide (Sigma Co.).

Induction of Femoral Fracture with the Periosteum Cauterized and Cell Transplantation

Female athymic nude rats (F344/N Jcl rnu/rnu; CLEA Japan, Inc.), age 8 to 12 weeks and weighing 150 to 170 g, were used in this study. The rats were fed a standard maintenance diet and provided with water *ad libitum*. The institutional animal care and use committees of Riken Center for Developmental Biology approved all animal procedures including human cell transplantation.

All surgical procedures were performed under anesthesia and normal sterile conditions. Anesthesia was performed with ketamine hydrochloride (60 mg/kg) and xylazine hydrochloride (10 mg/kg) administered intraperitoneally. A lateral parapatellar knee incision on the right limb was made to expose the distal femoral condyle. An animal model of femoral fracture was applied using a modification of the method described by Bonnarens and Einhorn.[23] To avoid significant displacement of the fracture by obtaining the well-aligned stability of the fracture site, a 1.2-mm-diameter K-wire was inserted from the trochlear groove into the femoral canal in a retrograde manner using a motor-driven drill. The wire was advanced until its proximal end was positioned stably in the greater trochanter, and the distal end was cut close to the articular surface of the knee. A thin saw cut at a depth of a 3 mm was applied mid-shaft after minimal lateral exposure to weaken the bone and to avoid complex fractures. A transverse femoral shaft fracture was then produced in the right femur of each rat using a C-shaped instrument applying three-point bending. After this procedure, each rat received additional surgery to produce a nonunion in the fractured shaft according to the method of Kokubu and colleagues.[24] The periosteum was cauterized (OPTEMP, variable low temperature cautery; Alcon Manufacturing, Ltd., Fort Worth, TX) circumferentially at a distance of 2 mm on each side of the fracture. The wound was then irrigated with 10 ml of sterile saline, and the muscle and skin were closed in layers with 5-0 nylon sutures. Postoperative pain was managed by administration of subcutaneous injection of buprenorphine hydrochloride after surgery. Unprotected weight bearing was allowed immediately after operation. The left unfractured femur served as a control. Thirty minutes after the production of the fracture, rats received an intravenous transplantation of 1×10^5 $CD34^+$ cells or 1×10^5 total MNCs resuspended with 100 μl of PBS or the same volume of PBS without cells through their tail vein ($n = 15$ in each group).

Three rats were randomly selected from each group and sacrificed for the histological study after radiological evaluation of fracture healing at each time point: weeks 2, 4, and 8. The six remaining rats in each group were sacrificed at week 8 for biomechanical testing as described below. If the fracture was not a stable transverse fracture or if any evidence of deep infection was seen, the animals were excluded from the study and replaced with additional animals. Thus, eight rats with comminuted fractures and six rats with infection identified by radiographs were replaced during the experiment.

Targeting Cell Analysis with Qtracker Cell Labeling Kit

To target human $CD34^+$ cells or MNCs after intravenous infusion and confirm their recruitment into fracture site, Qtracker 655 cell labeling kit (Quantum Dot Corp.) was applied for the human cells before transplantation in three additional rats in each group according to the manufacturer's instructions. In brief, Qtracker cell labeling kits deliver fluorescent quantum dot (qdot) nanocrystals into the cytoplasm of live cells using a custom targeting peptide and the long-term stability and brightness of qdots make them ideal candidates for live cell targeting and imaging.[25,26] The 1×10^5 $CD34^+$ cells or MNCs were incubated for 60 minutes with the Qtracker labeling solution (1 μl of Qtracker regent A and B) and 0.2 ml of Dulbecco's modified Eagle's medium in eight-well Lab-Tek chambered coverglass system. The cells were washed twice with Dulbecco's modified Eagle's medium and cell labeling was confirmed under fluorescence microscopy. The labeled cells were intravenously transplanted into each animal 30 minutes after fracture. All animals were sacrificed at day 7 for targeting cell analysis with Qtracker.

Reverse Transcriptase-Polymerase Chain Reaction (RT-PCR) Analysis of RNA Isolated from $CD34^+$ Cells and Peri-Fracture Site Tissue

Total RNA was obtained from the human $CD34^+$ cells immediately after isolation and from the rat tissues in peri-fracture site at day 14 using Trizol (Life Technologies) according to the manufacturer's instructions. The first-strand cDNA was synthesized using the RNA LA PCR kit version 1.1 (Takara), amplified by Taq DNA polymerase (Advantage-GC cDNA PCR kit; Clontech, Palo Alto, CA; and AmpliTaq Gold DNA polymerase; Applied Biosystems, Foster City, CA). PCR was performed using a PCR thermocycler (MJ Research PTC-225). Human CD31 (hCD31), human VE-cadherin (hVE-cad), human osteocalcin (hOC), human collagen1A1 (hCol1A1), human vascular endothelial growth factor (hVEGF), human fibroblast growth factor 2 (hFGF2), and human hepatocyte growth factor (hHGF) were amplified by *Taq*DNA polymerase (Advantage-GC cDNA PCR kit; Clontech) in the following conditions: 35 cycles of 30-second initial denaturation at 94°C, annealing at 56°C for 1 minute, and 30 seconds of extension at 72°C according to the manufacturer's instructions. Subsequently, PCR products were visualized in 1.5% ethidium bromide-stained agarose gels. Human umbilical vein endothelial cells and

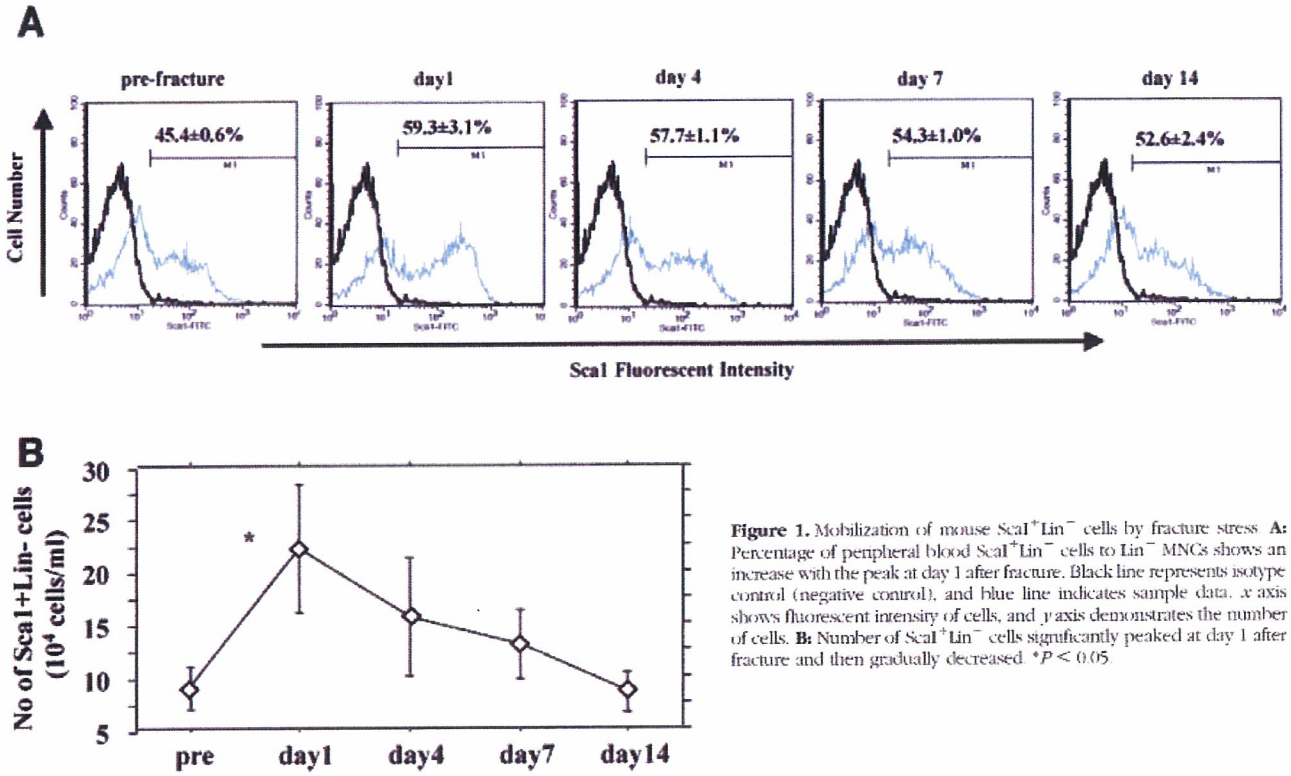

Figure 1. Mobilization of mouse Sca1$^+$Lin$^-$ cells by fracture stress. **A:** Percentage of peripheral blood Sca1$^+$Lin$^-$ cells to Lin$^-$ MNCs shows an increase with the peak at day 1 after fracture. Black line represents isotype control (negative control), and blue line indicates sample data. *x* axis shows fluorescent intensity of cells, and *y* axis demonstrates the number of cells. **B:** Number of Sca1$^+$Lin$^-$ cells significantly peaked at day 1 after fracture and then gradually decreased. $^*P < 0.05$.

hOBs (NHOst cells; Cambrex Bio Science, Walkersville, MD) were used for the positive control for human-specific endothelial and bone-related genes.

Primers

To avoid interspecies cross-reactivity of the primer pairs between human and rat genes, we designed the following human-specific primers using Oligo software (Takara). None of the primer pairs showed any cross-reactivity to rat genes (data not shown). hCD31 primer sequence (363 bp): sense 5′-ATCGATCAGTGGAACTTTGCCTATT-3′; anti-sense 5′-GTGGCATTTGAGATTTGATAGA-3′; hVE-cad primer sequence (461 bp): sense 5′-ACGCCTCTGTCATGTACCAAATCCT-3′; anti-sense 5′-GGCCTCGACGATGAAGCTGTATT-3′; hOC primer sequence (417 bp): sense 5′-AAGCAAGTAGCGCCAATCT-3′; anti-sense 5′-GGAAGTAGGGTGCCATAACAC-3′; hCol1A1 primer sequence (502 bp): sense 5′-CCTGGCCCCATTGGTAATGTT-3′; anti-sense 5′-CCCCCTCACGTCCAGATTCAC-3′; hVEGF primer sequence (186 bp): sense 5′-CAACATCACCATGCAGATTATGC-3′; anti-sense 5′-CCACAGGGACGGGATTTCTTG-3′; hFGF2 primer sequence (282 bp): sense 5′-AGCACAGTAACACTATCCTGCA-3′; anti-sense 5′-AAACGGAAACGCTCACCATAA-3′; hHGF primer sequence (282 bp): sense 5′-ACGAACACAGCTATCGGGGTA-3′; anti-sense 5′-CATCAAAGCCCTTGTCGGGAT-3′; hGAPDH primer sequence (596 bp): sense 5′-CTGATGCCCCCATGTTCGTC-3′; anti-sense 5′-CACCCTGTTGCTGTAGCCAAATTCG-3′; and rGAPDH primer sequence (320 bp): sense 5′-GTGCCAGCCTCGTCTCATAGA-3′; anti-sense 5′-CGCCAGTAGACTCCACGACAT-3′.

Single-Cell PCR

Single-CD34$^+$ cells derived from peripheral blood using the MACS system were put individually into PCR tubes with 4.5 μl of lysis buffer containing 50 mmol/L Tris-HCl, 75 mmol/L KCl, 5 U of SuperRNaseIN (Ambion), 7.5 U of PrimeRNase inhibitor (Eppendorf), 0.5% Nonidet P-40, 1 mmol/L dithiothreitol, 50 μmol/L dNTP, and 15 nmol/L MO-dT30 primer (5′-AAGCAGTGGTATCAACGCAGAGTGGCCATTACGGCCGTACTT-(dT)$_{30}$-3′). Tubes were then incubated at 65°C for 2 minutes and cooled to 45°C for 2 minutes. Reverse transcription was then performed by the addition of 100 U of SuperScript III (Invitrogen). After incubation at 45°C for 15 minutes, the reaction was terminated by heating at 65°C for 10 minutes. Next, 1.5 μl of RNA digestion mixture, 2 U of RNase H (Invitrogen), and 25 mmol/L $MgCl_2$ was added into each tube, and RNA digestion was performed by incubating at 37°C for 15 minutes and then inactivating at 65°C for 10 minutes. After RNA digestion, 6.5 μl of reaction mixture [5× terminal transferase buffer (Roche), 3 mmol/L $CoCl_2$, 1.5 mmol/L dATP, and 15 U of TdT (Promega)] was added, poly(A) tailing was performed by incubating at 37°C for 15 minutes, and inactivation was performed at 65°C for 10 minutes. cDNA amplification was performed using ExTaq polymerase (Takara Biochemicals, Japan). In brief, poly(A)-tailed cDNA (13 μl) was split 4 μl each into two tubes containing 16 μl of primary PCR reaction solution containing ExTaq PCR buffer (Takara Biochemicals), 2 mmol/L dNTP, 10 μmol/L MO-dT30 primer, and 1 U of ExTaq polymerase (Takara Biochemicals). PCR was performed with one cycle of 1 minute at 94°C, 2 minutes at 50°C, and 2 minutes at 72°C, followed by 35 cycles of

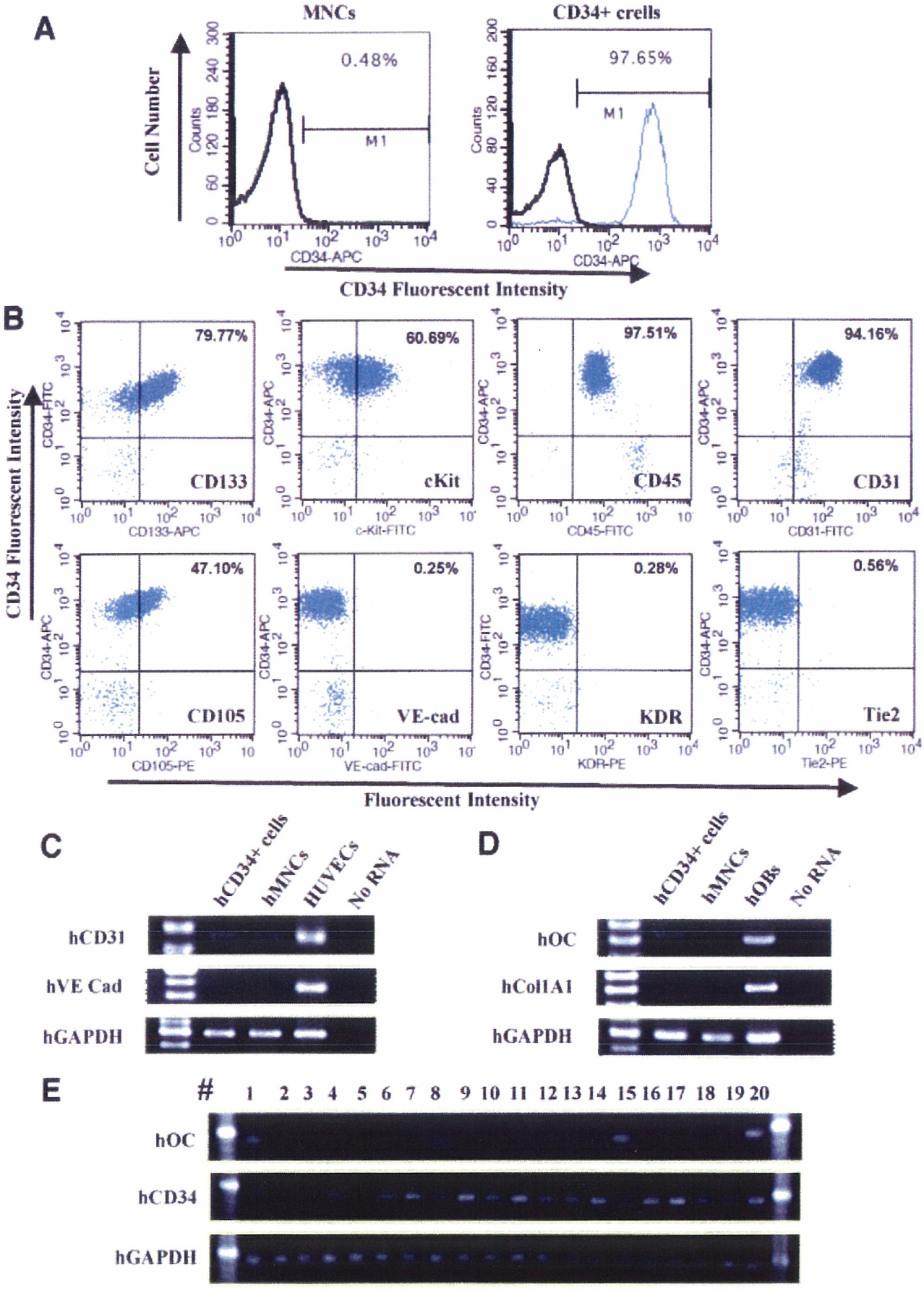
A
MNCs
CD34+ crells
0.48%
97.65%
M1
Cell Number
Counts
CD34-APC
CD34 Fluorescent Intensity
B
79.77%
CD133
60.69%
cKit
97.51%
CD45
94.16%
CD31
47.10%
CD105
0.25%
VE-cad
0.28%
KDR
0.56%
Tie2
CD34 Fluorescent Intensity
Fluorescent Intensity
C
hCD34+ cells
hMNCs
HUVECs
No RNA
hCD31
hVE Cad
hGAPDH
D
hCD34+ cells
hMNCs
hOBs
No RNA
hOC
hColIA1
hGAPDH
E
1 2 3 4 5 6 7 8 9 10 11 12 13 14 15 16 17 18 19 20
hOC
hCD34
hGAPDH

30 seconds at 94°C, 30 seconds at 60°C, and 2 minutes at 72°C. After combining split tubes into one tube, 2 μl of first-amplified cDNA was added to 18 μl of second PCR mixture, ExTaq PCR buffer (Takara Biochemicals), 2 mmol/L dNTP, 2 μmol/L MO-dT30 primer, and 1 U of ExTaq polymerase (Takara Biochemicals), and second PCR was performed for 35 cycles of 30 seconds at 94°C, 30 seconds at 60°C, and 2 minutes at 72°C. Finally, amplified cDNA purified with Qiagen PCR purification kit according to the manufacturer's procedure, and then PCR analysis for specific gene expression was performed using each purified cDNA.

Primers

hCD34 primer sequence (91 bp): sense 5′-TGCCTCT-TCTGTGGGTGACC-3′; anti-sense 5′-TCCAACCGTCAT-TGAAACCAG-3′; hOC primer sequence (96 bp): sense 5′-GCTCAATCCGGACTGTGACG-3′; anti-sense 5′-CA-GAGCGACACCCTAGACCG-3′; hGAPDH primer sequence (95 bp): sense 5′-GCATTGCCCTCAACGACC-3′; anti-sense 5′-CATGTGGGCCATGAGGTCC-3′.

Tissue Harvesting

Rats were euthanized with an overdose of ketamine and xylazine. Bilateral femurs were harvested and quickly embedded in optimal cutting temperature compound (Miles Scientific, Elkhart, IN), snap-frozen in liquid nitrogen, and stored at −80°C for histochemical and immunohistochemical staining as described below. Rat femurs in optimal cutting temperature blocks were sectioned, and 6-μm serial sections were mounted on silane-coated glass slides and air-dried for 1 hour before being fixed with 4.0% paraformaldehyde at 4°C for 5 minutes and stained immediately.

Morphometric Evaluation of Capillary Density and OB Density

Histochemical staining (n = 3 in each group) for isolectin B4 (Vector Laboratories, Burlingame, CA) as a rat EC marker or OC (Santa Cruz Biotechnology, Santa Cruz, CA) as a rat OB marker was visualized with diaminobenzidine (Vector Laboratories), and capillary or OB density was morphometrically evaluated as the average value in five randomly selected fields of soft tissue in the peri-fracture site (Figure 3M, zones a and b). To address the location of chondrocytes in the fractured sections, toluidine blue was used for counter staining. Capillaries were recognized as tubular structures positive for isolectin B4. OBs were recognized as lining or floating cells positive for OC on new bone surface. All morphometric studies were performed by two examiners blind to treatment.

Physiological Assessment of Tissue Perfusion by Laser Doppler Perfusion Imaging

Laser Doppler perfusion imaging (LDPI) (n = 3 in each group) (Moor Instrument, Wilmington, DE)[27,28] was used to measure serial blood flow in both legs throughout the course of 2 weeks after fracture. The ratio of fractured/intact (contralateral) blood flow was calculated to evaluate the serial blood flow recovery after fracture. The measurement was done under anesthesia with the animals supine and both limbs fully extended.

Immunofluorescent Staining

To detect transplanted human cells in the rat fracture site, immunohistochemistry (n = 3) was performed with the following human-specific antibodies: human leukocyte antigen (HLA)-ABC (BD Pharmingen) to detect various kind of human cells, hCD31 (DAKO, Glostrup, Denmark) for human ECs, and hOC (Biogenesis) for human OBs. Staining specificity for human cells without cross reaction to rat cells was confirmed by histochemical staining for HLA-ABC, hCD31, and hOC using human and rat heart or bone samples (data not shown). Double immunohistochemistry with HLA-ABC or hCD31 and smooth muscle actin (SMA) was performed to detect various human cells or human ECs in the arterioles. To estimate how many intravenously injected cells had recruited to the fracture site, the number of HLA-ABC-positive cells was morphometrically counted as the average value in five randomly selected soft tissue fields in the peri-fracture site. The secondary antibodies for each immunostaining were as follows: Alexa Flour 594-conjugated goat anti-mouse IgG_1 (Molecular Probes) for HLA-ABC and hCD31 staining and Alexa Flour 488-conjugated goat anti-mouse IgG_{2a} (Molecular Probes) for SMA. Immunohistochemistry with hOC was performed to detect human OBs along the newly formed bone surface. The secondary antibody for hOC is Cy3-conjugated AffiniPure goat anti-rabbit IgG (H^+L) (Jackson ImmunoResearch, West Grove, PA). 4,6-Diamidino-2-phenylindole (DAPI) solution was applied for 5 minutes for nuclear staining.

Inhibition of Neovascularization

To investigate the hypothesis that neovascularization is essential for supporting endogenous bone regeneration, we used an anti-angiogenic agent, soluble (s) Flt1 (VEGF receptor 1), known to inhibit proliferation of ECs.[29] First,

Figure 2. Phenotypic characterization of human peripheral blood MNCs and CD34$^+$ cells by FACS and RT-PCR analysis. **A:** FACS analysis to evaluate positivity for CD34 in MNCs (left) and CD34$^+$ cells (right). Numbers are percentages of the cells positive for CD34. **B:** FACS analysis to characterize CD34$^+$ cells by positivity for various cell surface markers. Human CD34$^+$ cells were positive for CD133, c-Kit, CD45, CD31, and CD105 and negative for VE-cad, KDR, and Tie2. Numbers are percentages of double-positive cells for CD34 (y axis) and each antibody (x axis). **C** and **D:** RT-PCR analysis for human-specific genes of endothelial (**C**) and osteoblastic (**D**) lineages was performed in freshly isolated CD34$^+$ cells and MNCs. The analysis of CD34$^+$ cells revealed weak expression of hCD31 and hOC but not of the other endothelial marker (hVE cad) or bone-related marker (hCol1A1). Cultured human umbilical vein endothelial cells and OBs were used for positive control for human-specific endothelial and bone-related genes. **E:** RT-PCR analysis at the single cell level of the CD34$^+$ cells. Four of 20 CD34$^+$ cells expressed both CD34 and hOC.

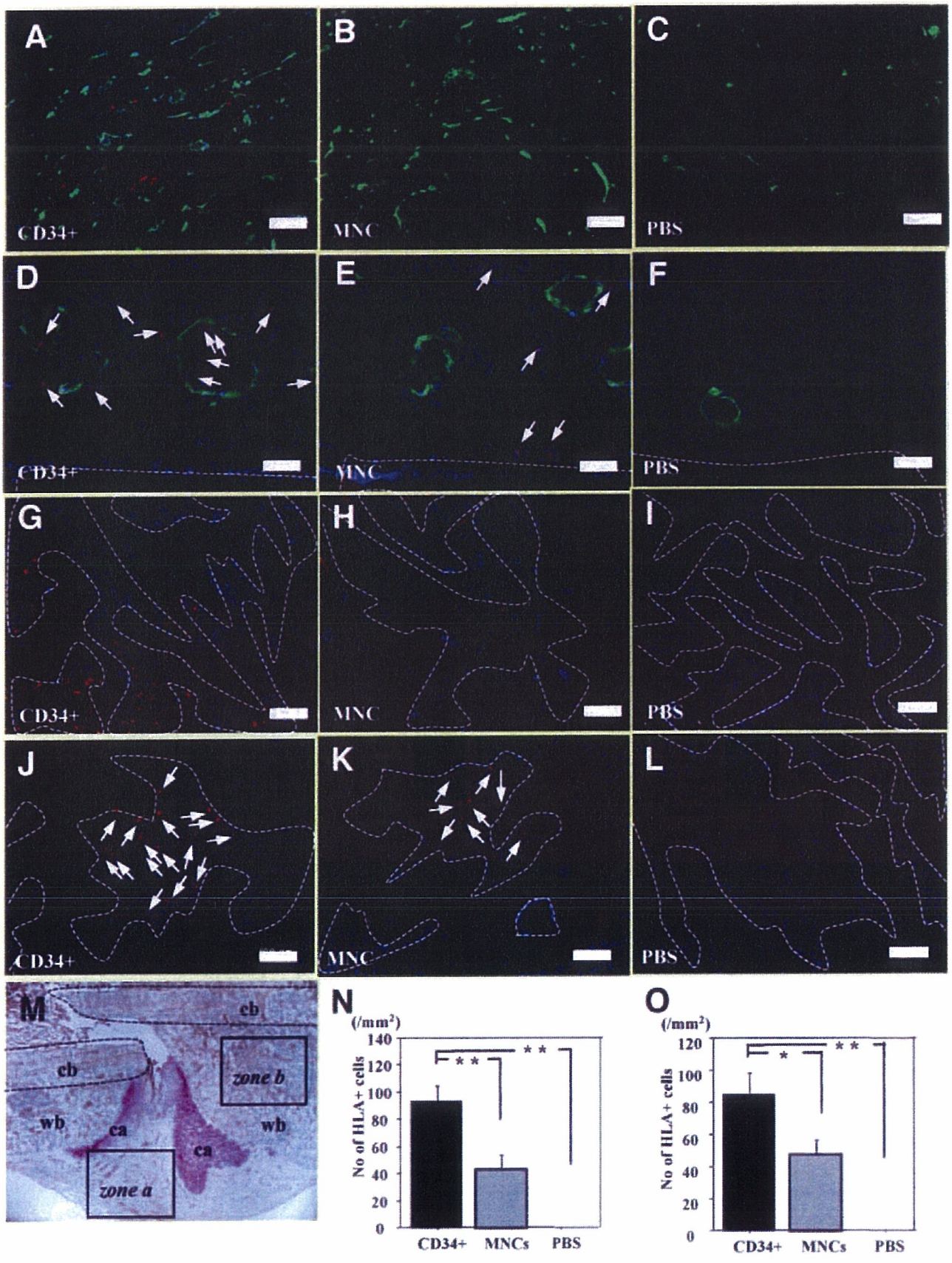
A
CD34+
B
MNC
C
PBS
D
CD34+
E
MNC
F
PBS
G
CD34+
H
MNC
I
PBS
J
CD34+
K
MNC
L
PBS
M
cb
cb
zone b
wb
ca
ca
wb
zone a
N
(/mm²)
No of HLA+ cells
140
120
100
80
60
40
20
0
* *
* *
CD34+
MNCs
PBS
O
(/mm²)
No of HLA+ cells
120
100
80
60
40
20
0
*
* *
CD34+
MNCs
PBS

we investigated whether transplanted human CD34$^+$ cells released angiogenic factors (hVEGF, hFGF2, hHGF) at the fracture site compared with the MNCs. Next, rats subjected to fracture and CD34$^+$ cell transplantation were divided into two groups; one group receiving sFlt1 (20 μg/kg, subcutaneous; R&D Systems, Minneapolis, MN) once daily for 14 days and the other receiving PBS only (n = 3 in each group). On day 14 after the cell transplantation, capillary and OB density, blood flow, and callus formation were assessed in each group.

Radiographical Assessment of the Fracture Healing

Radiographs of the fractured legs were serially taken at weeks 0, 2, 4, and 8 under anesthesia with the animal supine and both limbs fully extended. Fracture union was identified by the presence of bridging callus on two cortices. Radiographs of each animal were examined by three observers blinded to treatment. To evaluate the fracture healing process, callus formation was monitored radiographically, and relative callus areas detected by radiography were quantified with NIH Image (National Institutes of Health, Bethesda, MD) at week 2 in all groups.

Histological Assessment of the Fracture Healing

Histological evaluation (n = 3 in each group) was performed with toluidine blue staining to address the process of endochondral ossification at weeks 2, 4, and 8. The degree of fracture healing was evaluated at weeks 2, 4, and 8 in each group using a five-point scale proposed by Allen and colleagues[30] as follows: grade 4, complete bony union; grade 3, an incomplete bony union (presence of a small amount of cartilage in the callus); grade 2, a complete cartilaginous union (well-formed plate of hyaline cartilage uniting the fragments); grade 1, an incomplete cartilaginous union (retention of fibrous elements in the cartilaginous plate); and grade 0, the formation of a pseudoarthrosis (most severe form of arrest in fracture repair). All morphometric studies were performed by two orthopedic surgeons blind to treatment.

Biomechanical Assessment of the Fracture Union

At week 8, six rats in each treatment group were used for biomechanical evaluation.[31–34] After euthanasia, the fractured femurs and the contralateral nonfractured intact femurs were dissected free from the surrounding muscle. After the intramedullary K-wires were removed, a standardized three-point bending test was performed on the fractured site and on the same portion of the intact contralateral femur using a load torsion and bending tester (Computer Control System Shimazu Autograft; Simazu Co., Kyoto, Japan). The bending force was applied with cross-head at a speed of 2 mm/minute until fracture occurred. The ultimate stress (N/mm^2), the extrinsic stiffness (N/mm) and the failure energy (Nmm) were interpreted and calculated from the load deflection curve, which was recorded continuously in the computerized monitor linked to the tester. The percentage ratio of each parameter in the fractured (right) femur versus unfractured (left) femur was calculated in each animal.

Statistical Analysis

All values were expressed as mean ± SE. Paired Student's t-tests were performed for comparison of data before and after treatment. The comparisons among three groups were made using the one-way analysis of variance. Post hoc analysis was performed by Fisher's PLSD test. A probability value <0.05 was considered to denote statistical significance.

Results

Augmented Mobilization of Mouse Scal$^+$Lin$^-$ Cells by Fracture Stress

To confirm the kinetics of peripheral blood mouse Scal$^+$Lin$^-$ cells in the natural course of fracture healing, we serially performed FACS analysis to assess number of Scal$^+$Lin$^-$ cells in the peripheral blood after fracture. The MNCs obtained from the mice were 38.9 ± 4.8 × 10^4 cells, and the number of Lin$^-$ MNCs after lineage maker

Figure 3. Recruitment of fluorescent-labeled CD34$^+$ cells into fracture site. **A–C:** Histochemical staining for isolectin B4 (green), a rat-specific EC marker, using tissue samples of fracture sites obtained from rats receiving Qtracker-labeled human cells (red) 1 week after fracture in the granulation area shown as zone a in **M**. More efficient recruitment of human cells with neovasculature-like structure was accompanied with enhancement of neovascularization by recipient rat cells in animals treated with CD34$^+$ cells (**A**) compared with those receiving MNCs (**B**) or PBS alone (**C**). **D–F:** Double-fluorescent immunostaining for human leukocyte antigen (HLA)-ABC (red) and smooth muscle actin (green) using the tissue sample of granulation area. The massive recruitment of the human cells in the granulation area with relatively rare incorporation along the inner layer of SMA-positive smooth muscle cells was observed in CD34$^+$ group. The human cells lining along the inner layer were morphologically compatible with ECs (**D**). In contrast, less recruitment of human cells in the granulation area and no human cells along the inner layer of arterioles were observed in animals receiving MNCs (**E**). Human cells were not found in the PBS group (**F**). **G–I:** Pursuit of Qtracker-labeled human cells 1 week after fracture in newly formed bone area shown as zone b in **M**. Human cell (red) recruitment into the newly formed bone area (surrounded by broken lines) was more abundant in animals treated with CD34$^+$ cells (**G**) compared with those receiving MNCs (**H**) or PBS alone (**I**). **J–L:** Fluorescent immunohistochemistry for HLA-ABC demonstrated massive recruitment of human cells (red: **arrows**) in CD34$^+$ group (**J**). In contrast, less recruitment of the HLA-ABC-positive cells was observed in animals receiving MNCs (**K**) and no human cells in PBS group (**L**). **M:** Representative photomicrograph of immunostaining for isolectin B4 (brown) and toluidine blue counter staining for anatomical indication of following areas: zone a, granulation zone; zone b, newly formed bone zone; cb, cortical bone; ca, cartilage; wb, woven bone. **N:** The number of HLA-ABC-positive cells observed in zone a was significantly greater in CD34$^+$ group compared with other groups. $^{**}P < 0.01$. **O:** The number of HLA-ABC-positive cells in zone b was significantly greater in CD34$^+$ group compared with other groups. $^*P < 0.05$; $^{**}P < 0.01$. Blue fluorescence indicates DAPI for nuclear staining. Scale bars = 100 μm (**A–C, G–F**); 50 μm (**D–F, J–L**). Original magnifications: ×100 (**A–C, G–I**); ×200 (**D–F, J–L**); ×40 (**M**).

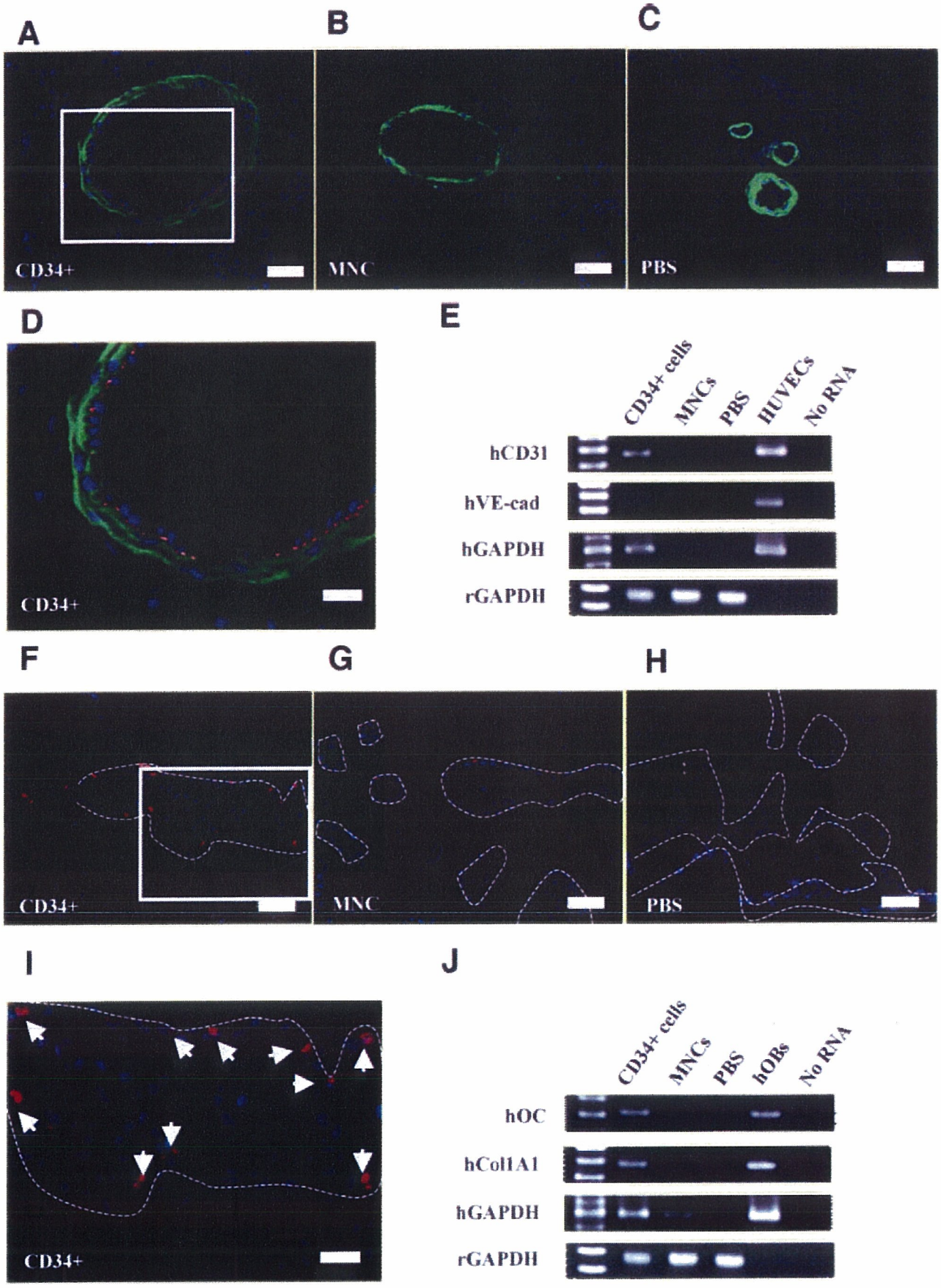
A
B
C
CD34+
MNC
PBS
D
E
CD34+
CD34+ cells
MNCs
PBS
HUVECs
No RNA
hCD31
hVE-cad
hGAPDH
rGAPDH
F
G
H
CD34+
MNC
PBS
I
J
CD34+
CD34+ cells
MNCs
PBS
hOBs
No RNA
hOC
hCol1A1
hGAPDH
rGAPDH

depletion by MACS system was 26.5 ± 3.0 × 10^4 cells. The percentage of peripheral blood Scal$^+$Lin$^-$ cells in relation to Lin$^-$ MNCs by FACS analysis had a tendency to peak at day 1 after fracture and gradually decrease thereafter; however, these changes were not statistically significant (prefracture, 45.4 ± 0.6; 1 day after fracture, 59.3 ± 3.1; 4 days after fracture, 57.7 ± 1.1; 7 days after fracture, 54.3 ± 1.0; 14 days after fracture, 52.6 ± 2.4%) (Figure 1A). The number of Scal$^+$Lin$^-$ cells, calculated from the number of Lin$^-$ MNCs and the percentage of Scal$^+$ cells in the number of Lin$^-$ MNCs, significantly increased at day 1 after fracture and then gradually decreased (prefracture, 8.3 ± 1.4; 1 day after fracture, 22.1 ± 6.1; 4 days after fracture, 15.6 ± 9.7; 7 days after fracture, 12.9 ± 5.7; 14 days after fracture, 8.4 ± 1.9 × 10^4 cells/ml; $P < 0.05$ for prefracture versus 1 day after fracture) (Figure 1B). These results indicate that mouse Scal$^+$Lin$^-$ cells, quite similar to human CD34$^+$ cells, were mobilized into the peripheral blood at an early phase of the fracture healing process.

Phenotypic Characterization of CD34$^+$ Cells Obtained from Adult Human Volunteers

Peripheral blood total mononuclear cells (MNCs) were obtained from healthy male volunteers, age 31.7 ± 1.2 years (n = 3), and CD34$^+$ cells were isolated from the MNCs by AutoMACS. The MNCs contained a CD34$^+$ cell fraction at the rate of <0.5% and the CD34$^+$ cell fraction had a purity of >97% as determined by FACS analysis (Figure 2A). The freshly isolated CD34$^+$ cells were also characterized as positive for cell surface markers of CD45, CD133, c-Kit, CD31, and CD105 (Figure 2B). RT-PCR analysis of the CD34$^+$ cells revealed weak expression of the human-specific genes, hCD31 and hOC, but not of another EC marker, hVE-cad, or another bone-related marker, hCol1A1 (Figure 2, C and D). RT-PCR analysis at the single cell level of the CD34$^+$ cells revealed that 4 of 20 CD34$^+$cells expressed hOC (Figure 2E). These results indicate that human peripheral blood CD34$^+$ cells contain not only endothelial progenitor but also osteo-progenitor cells.[19,35]

Massive Recruitment of CD34$^+$ Cells into the Fracture Site

To simulate the clinical situation of the nonhealed fracture, a reproducible model of femoral fracture[23] with cauterized periosteum, which led to nonunion 8 weeks after fracture,[12,24] was applied in nude rats. Human CD34$^+$ cells isolated from peripheral blood were labeled with the Qtracker cell labeling kit (Qtracker; Quantum Dot Corp.) and intravenously administered via the tail vein 30 minutes after fracture production. MNCs labeled with Qtracker or PBS alone were similarly infused into control animals. Rats were sacrificed 1 week after the cell infusion and then histochemical staining for isolectin B4, a rat-specific EC marker, was performed. Fluorescent microscopy demonstrated a massive recruitment of human cells with tubular structure, which were morphologically compatible with vascular cells, and the enhancement of neovascularization by rat ECs around the granulation area (Figure 3M, zone a) in animals treated with CD34$^+$ cells (CD34$^+$ group) (Figure 3A). In contrast, recruitment of human cells into this area was rarely observed in rats receiving MNCs, and augmentation of recipient vascularity was not obvious in animals receiving MNCs or PBS (Figure 3, B and C). To further confirm the human cell incorporation into the fracture site, especially into the arterioles, tissue samples were stained with HLA-ABC and SMA. The double immunostaining demonstrated the massive recruitment of the human cells in the granulation area with relatively rare incorporation along the inner layer of SMA-positive smooth muscle cells in CD34$^+$ group. The human cells lining along the inner layer were morphologically compatible with ECs (Figure 3D). In contrast, less recruitment of human cells in the granulation area and no human cells along the inner layer of arterioles were observed in animals receiving MNCs (Figure 3E). No human cells were found in the area of PBS group (Figure 3F). The number of human cells in the granulation area was significantly higher in the CD34$^+$ group compared with the other groups (CD34$^+$, 93.1 ± 11.3/mm^2; MNC, 43.1 ± 10.4/mm^2; PBS, 0.0 ± 0.0/mm^2, respectively; $P < 0.01$ for CD34$^+$ versus MNC or PBS group) (Figure 3N).

Fluorescent microscopy 1 week after the cell infusion also demonstrated abundant recruitment and distribution of human cells in the newly bone formed area (zone b in Figure 3M) as well as the granulation area in CD34$^+$ group (Figure 3G). In contrast, recruitment of human cells into zone b was rarely observed in other groups (Figure 3, H and I). To quantitatively assess the number of recruited cells, tissue samples were stained with HLA-ABC, and the number of HLA-ABC-positive cells was morphometrically counted in the newly formed bone area. Fluorescent microscopy demonstrated a massive recruitment of human cells in CD34$^+$ group (Figure 3J). In contrast, there was less recruitment of HLA-positive cells in animals receiving MNCs (Figure 3K) and no human cells were seen in the PBS group (Figure 3L). The number of HLA-ABC-positive cells in the newly formed bone area was significantly greater in the CD34$^+$ group compared with

Figure 4. Human CD34$^+$ cell-derived vasculogenesis and osteogenesis. Immunohistochemical staining and RT-PCR for human-specific EC or OB markers was performed using tissue samples harvested at week 2. **A–D:** Differentiated human ECs were identified in zone a as hCD31-positive cells (red) in animals receiving CD34$^+$ cells compared with MNC (**B**) or PBS group (**C**). **E:** RT-PCR analysis of tissue RNA isolated from the peri-fracture site demonstrated the expression of human-specific EC markers (hCD31, hVE-cad) in animals treated with CD34$^+$ cells but not in control animals. Cultured human umbilical vein endothelial cells were used for positive control, and no RNA served as negative control. **F–I:** Differentiated human OBs were identified in zone b as hOC-positive cells (red) in animals receiving CD34$^+$ cells compared with MNC (**G**) or PBS group (**H**). **J:** RT-PCR analysis of RNA isolated from the peri-fracture site demonstrates the expression of human-specific bone-related markers (hOC, hCol1A1) in animals treated with CD34$^+$ cells, but not in control animals. Cultured hOBs were used for positive control. Blue fluorescence represents DAPI. Broken lines, newly formed bone surface. Scale bars = 50 μm (**A–C, F–H**); 20 μm (**D, I**). Original magnifications: ×200 (**A–C, F–H**); ×400 (**D, I**).

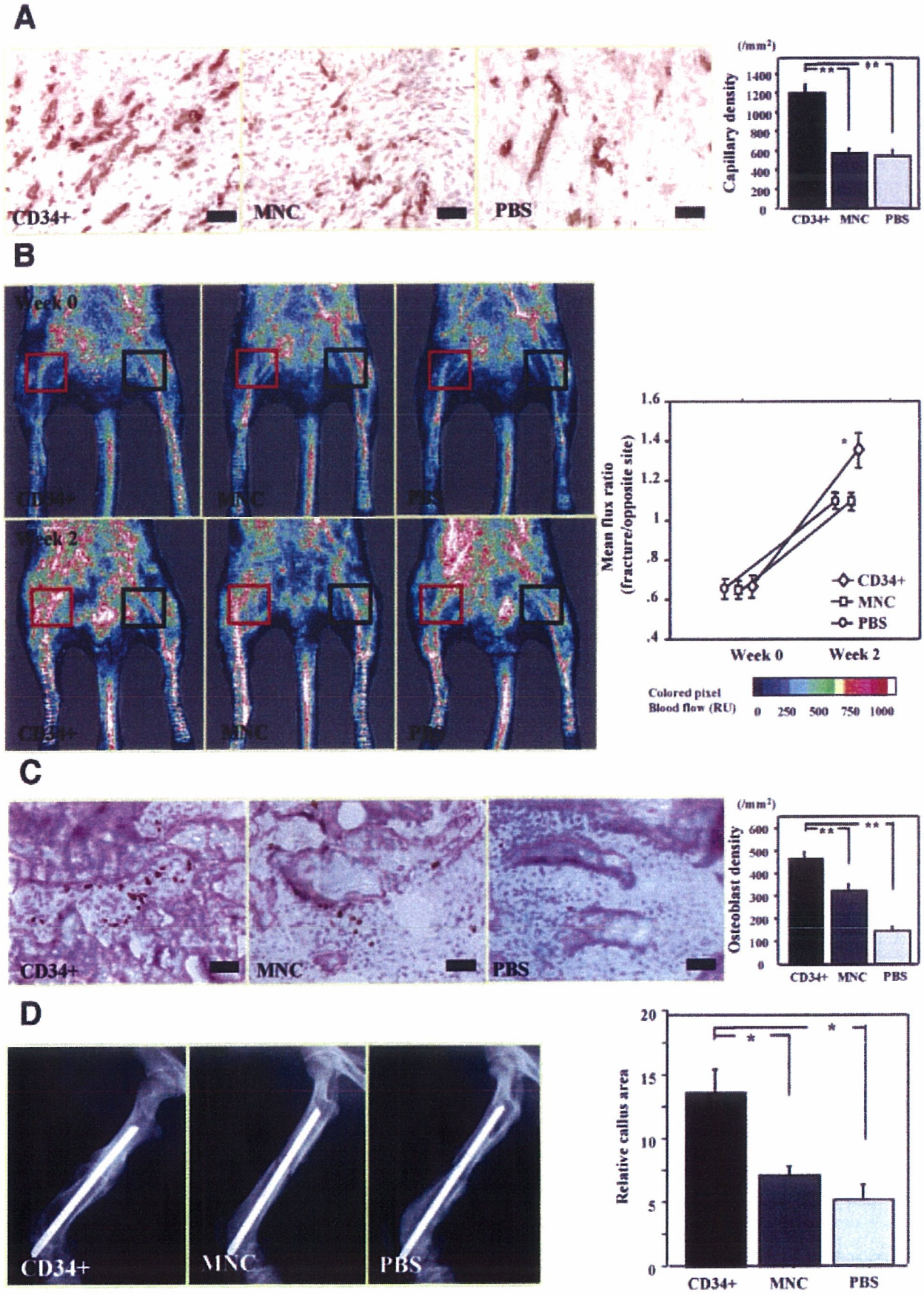
A
CD34+
MNC
PBS
(/mm²)
Capillary density
1400
1200
1000
800
600
400
200
0
**
**
CD34+ MNC PBS
B
Week 0
Week 2
CD34+
MNC
PBS
Mean flux ratio
(fracture/opposite site)
1.6
1.4
1.2
1
.8
.6
.4
*
CD34+
MNC
PBS
Week 0
Week 2
Colored pixel
Blood flow (RU)
0 250 500 750 1000
C
CD34+
MNC
PBS
(/mm²)
Osteoblast density
600
500
400
300
200
100
0
**
**
CD34+ MNC PBS
D
CD34+
MNC
PBS
Relative callus area
20
15
10
5
0
*
*
CD34+ MNC PBS

the other groups (CD34$^+$, 84.7 ± 13.5/mm^2; MNC, 47.2 ± 9.0/mm^2; PBS, 0.0 ± 0.0/mm^2 respectively; $P < 0.05$ for CD34$^+$ versus MNC, $P < 0.01$ for CD34$^+$ versus PBS group) (Figure 3O). These morphological findings indicate that human peripheral blood CD34$^+$ cells infused intravenously are recruited into not only the granulation zone but also the newly formed bone zone in the fracture healing process.

Human CD34$^+$ Cell-Derived Vasculogenesis and Osteogenesis

Next, we performed experiments to characterize the human cells recruited into the fracture sites. To histologically demonstrate the phenomenon of human cell-derived vasculogenesis, immunohistochemical staining for hCD31, a human-specific EC marker, was performed using tissue samples obtained 2 weeks after cell infusion. Differentiated human ECs derived from the transplanted CD34$^+$ cells were detected as hCD31$^+$ cells in the vasculature in the peri-fracture area (Figure 4, A and D), whereas hCD31$^+$ cells were not identified in the MNC (Figure 4B) or PBS group (Figure 4C). To further confirm this phenomenon in terms of transcription, RT-PCR analysis of tissue RNA isolated from the peri-fracture site was performed. The molecular approach revealed the gene expression of human-specific EC markers (hCD31 and hVE-cad) in the CD34$^+$ group, but not in the other groups (Figure 4E).

To identify human cell-derived osteogenesis, immunohistochemical staining for hOC, a human-specific OB marker was performed using tissue samples obtained 2 weeks after cell infusion. Human OBs derived from the transplanted CD34$^+$ cells were observed as lining cells along the newly formed bone surface (Figure 4, F and I), whereas only a few human OBs were identified in the MNC group (Figure 4G) and no human OBs were identified in the PBS group (Figure 4H). RT-PCR analysis of tissue RNA isolated from the peri-fracture site demonstrated the expression of human-specific bone-related markers (hOC and hCol1A1) in the CD34$^+$ group, but not in other groups (Figure 4J). These results indicate that human peripheral blood CD34$^+$ cells differentiate into both ECs and OBs in a fracture-induced environment.

Enhancement of Intrinsic Angiogenesis and Osteogenesis in Animals Receiving CD34$^+$ Cells

Enhanced angiogenesis and osteogenesis by recipient's cells after cell transplantation were further confirmed by immunostaining for rat-specific markers. Vascular staining with isolectin B4 (marker for rat EC, but not human) using tissue samples at week 2 after fracture demonstrated enhanced neovascularization around the granulation area (Figure 3M, zone a) in CD34$^+$ group compared with MNC or PBS group (Figure 5A). Neovascularization assessed by capillary density was significantly enhanced in CD34$^+$ group compared with the other groups (CD34$^+$, 1187.5 ± 79.3/mm^2; MNC, 562.5 ± 36.6/mm^2; PBS, 532.5 ± 49.3/mm^2, respectively; $P < 0.01$ for CD34$^+$ versus MNC or PBS group) (Figure 5A).

OB staining for rat-specific OC (marker for rat OB but not human) using tissue samples at week 2 after fracture revealed augmentation of osteogenesis in the area of new bone formation (Figure 3M, zone b) in animals treated with CD34$^+$ cells compared with those receiving MNCs or PBS alone (Figure 5C). Osteogenesis assessed by the OB density was significantly enhanced in CD34$^+$ group compared with other groups (CD34$^+$, 468.0 ± 25.3/mm^2; MNC, 321.6 ± 28.8/mm^2; PBS, 141.6 ± 14.0/mm^2, respectively; $P < 0.01$ for CD34$^+$ versus MNC or PBS group) (Figure 5C). These results indicate that administration of human CD34$^+$ cells enhances both intrinsic angiogenesis and osteogenesis by recipient cells.

Improvement of Blood Flow and Enhancement of Callus Formation in Animals Receiving CD34$^+$ Cells after Fracture

To evaluate blood flow recovery at the fracture site by physiological approach, LDPI was serially performed after fracture. LDPI analysis demonstrated severely low blood flow at the fracture sites 1 hour after fracture production and its recovery at week 2 in all groups (Figure 5B). The ratio of fractured/intact (contralateral) blood flow was significantly increased by week 2 in all groups (Figure 5B). There was no significant difference in the blood flow ratio 1 hour after fracture production among the groups, whereas the ratio at day 14 was significantly higher in CD34$^+$ group compared with the other groups (CD34$^+$, 1.344 ± 0.079; MNC, 1.096 ± 0.037; PBS, 1.085 ± 0.024, respectively; $P < 0.05$ for CD34$^+$ versus MNC or PBS group) (Figure 5B).

To evaluate the fracture healing process, callus formation was monitored radiographically and the relative callus area detected by radiography was quantified with NIH Image at week 2 in all groups (Figure 5D). The relative callus area was significantly larger in the CD34$^+$ group

Figure 5. Enhanced intrinsic vascularization and osteogenesis by recipient's cells and serial improvement of blood flow and enhancement of callus formation after CD34$^+$ cell transplantation. **A:** Rat-specific vascular staining with isolectin B4 (brown) at week 2 demonstrated enhanced neovascularization in zone a in animals treated with CD34$^+$ cells compared with those receiving MNCs or PBS alone. Intrinsic angiogenesis assessed by capillary density at week 2 was significantly enhanced after CD34$^+$ cell transplantation compared with other treatments. $^{**}P < 0.01$. **B:** Representative LDPI at week 0 (1 hour after fracture) and week 2 in each group. In these digital color-coded images, maximum perfusion values are indicated in white, medium values in green to yellow, and lowest values in dark blue. The skin blood flow within fracture site (**red square**) and intact contralateral site (**black square**) were evaluated as mean flux, and ratio of the mean flux in the fractured site with that in the contralateral site (mean flux ratio) was calculated. Severe reduction of the blood flow was similarly observed 1 hour after fracture with the periosteum cauterized in all groups, whereas the mean flux ratio at week 2 was significantly greater in animals treated with CD34$^+$ cells compared with those receiving MNCs or PBS alone. $^*P < 0.05$. **C:** Rat-specific OC staining (brown) to detect intrinsic OBs at week 2 revealed augmentation of osteogenesis in zone b in animals treated with CD34$^+$ cells compared with those receiving MNCs or PBS alone. Intrinsic osteogenesis assessed by the OB density at week 2 was significantly enhanced after CD34$^+$ cell transplantation compared with other groups. $^{**}P < 0.01$. **D:** Relative callus area assessed by radiograph at week 2 was significantly larger in CD34$^+$ group compared with other groups. $^*P < 0.05$. Scale bars = 50 μm. Original magnifications, ×200.